

Fluorescence-based screens for identifying small-molecule activators of Parkin

Andrea Krahn

Integrated Program in Neuroscience

McGill University, Montreal

April 2018

A thesis submitted to McGill University in partial fulfillment of the requirements of the degree

of Master of Science

© Andrea Krahn, 2018

Table of Contents

Abstract	3
Résumé	4
Acknowledgements	5
Preface and Contribution of Authors	6
List of Abbreviations	7
Introduction and Rationale	8
Background	9
Aims	16
Methods	17
Results	22
Discussion	26
Conclusion	29
References	31
Figures	37
Supplemental Figures	43

Abstract

Parkinson's disease (PD) is a neurodegenerative disease characterized by the selective and progressive degeneration of dopaminergic neurons in the substantia nigra (SN). While the underlying cause of neurodegeneration is unknown, mitochondrial dysfunction has been identified as a potential cause of PD. Most PD cases are idiopathic, with familial forms accounting for less than ten percent of PD cases. Nevertheless, the identification of rare, inheritable variants of the disease has increased our understanding of PD etiology. More specifically, loss-of-function mutations in the *PARK2* gene, which encodes the E3 ubiquitin (Ub)-ligase Parkin, have been linked to autosomal-recessive juvenile parkinsonism (ARJP). Parkin, along with PTEN-induced putative kinase 1 (PINK1), another PD-associated protein, mediate the removal of dysfunctional mitochondria through a specialized form of autophagy. X-ray crystallography, however, has revealed that Parkin is auto-inhibited in its basal state and requires extensive conformational rearrangement to exhibit E3 ligase activity. These structural changes can be monitored using fluorescent probes, that can be used to guide the discovery of small-molecule activators of Parkin. We have developed three fluorescence-based assays to monitor Parkin activity. The first assay detects the transfer of Ub onto Parkin as a direct consequence of Parkin activation. The second is a cell-based assay that monitors specific conformational changes in Parkin during activation using Förster resonance energy transfer (FRET). The third is a modified *in vitro* FRET assay that can be used to validate small-molecule activators of Parkin. Since Parkin exhibits neuroprotective activity, activators of Parkin have the potential to slow down or stop the progression of PD.

Résumé

La maladie de Parkinson (MP) est une maladie neurodégénérative caractérisée par la dégénérescence progressive des neurones dopaminergiques de la substance noire. Tandis que l'agent causant la neurodégénérescence est inconnu, la dysfonction mitochondriale a été identifiée comme une cause potentielle de la MP. La plupart des cas de MP sont idiopathiques, et les formes familiales représentent moins de 10% des cas. Cependant, l'identification de variants rares et héréditaires de la MP ont amélioré notre compréhension de son étiologie. Plus précisément, des mutations causant une perte-de-fonction du gène *PARK2*, qui encode l'ubiquitin (Ub)-ligase E3 Parkin, ont été liées au parkinsonisme autosomal-récessif juvénile. Parkin agit avec la kinase putative 1 induite par PTEN (PINK1), elle aussi associée à la MP, pour contrôler l'élimination des mitochondries dysfonctionnelles *via* une forme spécialisée d'autophagie. La cristallographie aux rayons X a cependant révélé que Parkin est auto-inhibée dans son état basal, et requiert un réarrangement conformationnel majeur afin d'exhiber son activité ligase. Ces changements structuraux peuvent être monitorés avec des sondes fluorescentes, guidant la découverte de petites molécules activatrices de Parkin. Nous avons développé trois essais basés sur la fluorescence pour monitorer l'activité de Parkin. Le premier, *in vitro*, peut détecter le transfert de l'Ub sur Parkin comme conséquence directe de l'activation de Parkin. Le second mesure, par transfert d'énergie par résonance Förster (FRET) *in cellulo*, les changements conformationnels subis par Parkin au cours de son activation. Le troisième est une version modifiée de FRET *in vitro* qui peut être utilisé pour valider des petites molécules activatrices de Parkin. Puisque Parkin a une activité neuroprotectrice, des activateurs de Parkin ont le potentiel de ralentir ou d'abolir la progression de la MP.

Acknowledgements

First and foremost, I would like to thank my supervisor Dr. Edward Fon for giving me the opportunity to undertake this project at the Montreal Neurological Institute and for helping me grow as a scientist. My utmost gratitude goes to Matthew Tang, who took the time to train me in all the laboratory techniques necessary for the completion of this thesis. To all the members of the Fon lab for useful discussion and comments during our lab meetings, and for all the fun hours spent outside of the lab as social butterflies.

A huge thank you to Dr. Jean-François Trempe and Marta Vranas for becoming major contributors to this project by providing their extensive knowledge in protein structure. I would also like to acknowledge Dr. Kalle Gehring and Dr. Heidi McBride, my committee members, for all the scientific brainstorming and valuable insights into my project.

Financial assistance for this project was provided by Dr. Fon through the Canadian Institutes of Health Research (CIHR), the Michael J. Fox Foundation (MJFF), and Merck Sharp & Dohme (MSD).

To Cheryl Collucci, my mentor at AAFC and CCIW, for teaching me the right way to do things and making me the researcher I am today. Shout out to Lawrie for helping me stay on track with all my thesis deadlines, and to Erika for countless caffeinated hours spent motivating me to write. Lastly and most importantly, I am ever so grateful to my family and friends for keeping me sane throughout the emotional rollercoaster of academia. Their love and support have more impact on my work than they can imagine.

Preface and Contribution of Authors

The aim of this thesis was to develop fluorescence-based assays to study Parkin activation. These assays have the potential to be used as screening tools for the discovery of small-molecule activators that could be developed into therapeutic treatments for PD. The majority of the work done characterizing our *HsParkin* FRET reporters has already been published in *Nature Communications* (Tang et al., 2017).

The author generated the text, data, and figures in this thesis, except where indicated here. Dr. Edward Fon and Dr. Heidi McBride participated in the design of the auto-ubiquitination assay. Design of the FRET assays was conceptualized by Dr. Edward Fon, Dr. Jean-François Trempe, and Dr. Matthew Tang. Dr. Matthew Tang analyzed the FACS data and generated the images for the cell-based FRET data. Mass spectrometry analysis was performed by Dr. Jean-François Trempe. Dr. Marta Vranas subcloned the *HsParkin* FRET reporters into pGEX-6P-1 and performed the *in vitro* auto-ubiquitination of the recombinant *HsParkin* FRET reporters. FRET analysis performed on the high-content systems was done by Dr. Wolfgang Reintsch. Cloning of constructs, purification of recombinant proteins, generation of stable cell lines, protein labelling and phosphorylation, auto-ubiquitination experiments, and data analysis were performed by the author. Parkin recruitment and mitophagy assays were performed by both the author and Dr. Matthew Tang.

The Flow Cytometry and Cell Sorting Facility at the Duff Medical Building of McGill provided assistance with the FACS experiments; the facility's infrastructure is supported by the Canada Foundation for Innovation (CFI).

List of Abbreviations

- aa, amino acid
- Akt, Protein Kinase B
- ARJP, Autosomal-recessive juvenile parkinsonism
- ATP, Adenosine triphosphate
- CCCP, Carbonyl cyanide *m*-chlorophenyl hydrazone
- CFP, Cyan fluorescent protein
- DA, Dopamine
- DNA, Deoxyribonucleic acid
- DTT, Dithiothreitol
- eGFP, Enhanced green fluorescent protein
- EGFR, Epidermal growth factor receptor
- Eps15, Epidermal growth factor receptor substrate 15
- FACS, Fluorescence-activated cell sorting
- FPLC, Fast protein liquid chromatography
- FRET, Förster resonance energy transfer
- GSH, Glutathione
- GST, Glutathione S-transferase
- HCS, High-content screening
- HECT, Homologous to the E6-AP carboxyl terminus
- HEPES, 4-(2-hydroxyethyl)-1-piperazineethanesulfonic acid
- IPTG, Isopropyl- β -D-thiogalactoside
- LB, Lysogeny broth
- LC3, Microtubule-associated proteins 1A/1B light chain 3B
- LUBAC, Linear ubiquitin assembly complex
- MDV, Mitochondrial-derived vesicle
- Mfn, Mitofusin
- MPP+, 1-methyl-4-phenylpyridinium
- MPTP, 1-methyl-4-phenyl-1,2,3,6-tetrahydropyridine
- mtKeima, Mitochondrially targeted Keima
- NBR1, Neighbor of BRCA1 gene 1 protein
- NDP52, Nuclear domain 10 protein 52
- NEMO, NF- κ B essential modulator
- NF- κ B, Nuclear factor kappa-light-chain-enhancer of activated B cells
- OPA1, Dynamin-like 120 kDa protein
- OPTN, Optineurin
- p62, Nucleoporin p62
- PARIS, Parkin-interacting substrate
- PBS, Phosphate-buffered saline
- PCR, Polymerase chain reaction
- PD, Parkinson's disease
- PGC1 α , Peroxisome proliferator-activated receptor gamma co-activator 1-alpha
- PINK1, PTEN-induced putative kinase 1
- PTEN, Phosphatase and tensin homolog
- pUb, Phosphorylated ubiquitin
- RBR, RING-between-RING
- REP, Repressor element of Parkin
- RING, Really interesting new gene
- ROS, Reactive oxygen species
- SN, Substantia nigra
- TBS, Tris-buffered saline
- U2OS, Human osteosarcoma
- Ub, Ubiquitin
- Ubl, Ubiquitin-like
- WT, Wild type
- YFP, Yellow fluorescent protein

Introduction and Rationale

PD is a debilitating disease that affects an increasing number of patients due to the demographic trend towards an aged population (de Rijk et al., 2000). It is characterized by the selective and progressive degeneration of dopaminergic neurons in the SN, resulting in classical clinical motor symptoms that include bradykinesia, rigidity, postural instability, and resting tremor (Lang and Lozano, 1998a; Lang and Lozano, 1998b). It has been proposed that the extensive arborized axonal architecture of DA neurons in the SN results in high metabolic demands, leading to increased production of reactive oxygen species (ROS), damaging mitochondria and eventually resulting in neuronal cell death (Bolam and Pissadaki, 2012; Matsuda et al., 2009; Pacelli et al., 2015; Pissadaki and Bolam, 2013).

While the majority of PD cases are sporadic, ten percent of PD cases have underlying genetic causes. Specifically, juvenile parkinsonism has been linked to autosomal mutations in the genes that encode Parkin and PINK1 (Kitada et al., 1998; Valente et al., 2004). These two proteins act in concert to selectively target damaged mitochondria for degradation by a form of autophagy termed mitophagy. The crystal structure of Parkin revealed that it adopts an auto-inhibited conformation under basal conditions, with several sites of inhibition (Trempe et al., 2013). While the active structure of Parkin has yet to be solved, it is hypothesized that several conformational changes must occur for Parkin to be fully active.

Our laboratory has designed three fluorescence-based assays to monitor Parkin activity that could be used as potential screening tools to identify small-molecule activators of Parkin. The first is an auto-ubiquitination assay that detects the transfer of fluorescently-labelled Ub onto Parkin as a direct consequence of Parkin activation. Higher fluorescence intensities should correlate with increasing amounts of Ub bound to Parkin, which would suggest greater E3 ligase activity. The

second is a structure-based Förster resonance energy transfer (FRET) assay that can monitor specific conformational changes that occur in Parkin upon activation. We have shown that point mutations designed to depress Parkin's auto-inhibited conformation, which correlated with an increased E3 ligase activity as well as an accelerated rate of recruitment to the mitochondria, resulted in FRET efficiency changes (Tang et al., 2017). Compounds that are capable of activating Parkin are expected to result in FRET efficiency changes in our cell-based FRET assay. The third is a modified *in vitro* FRET assay that can be used to validate small-molecule activators of Parkin. Compounds that activate Parkin through direct binding should result in FRET efficiency changes. Since Parkin exhibits neuroprotective activity, small-molecule compounds that activate Parkin have the potential to be developed into PD therapeutic agents that could prevent or delay the progression of the disease.

Background

Parkinson's Disease

PD is the most common movement disorder and the second most common neurodegenerative disease after Alzheimer's disease. It is pathologically characterized by the selective and progressive degeneration of dopaminergic neurons in the substantia nigra (SN) that project to the striatum in the basal ganglia. Depletion of striatal dopamine (DA) results in classical clinical motor symptoms that include bradykinesia, rigidity, postural instability, and resting tremor (Lang and Lozano, 1998a; Lang and Lozano, 1998b). The remaining SN neurons typically contain proteinaceous inclusions, termed Lewy bodies, which are mainly composed of α -synuclein (Spillantini et al., 1998). Aside from the motor symptoms of PD, patients exhibit non-motor features such as sleep disorders, loss of sense of smell, cognitive changes, and mood disorders, which contribute to a systemic and heterogeneous syndrome (Schapira et al., 2017).

Parkin and PINK1 mutations are linked to familial forms of PD

While the majority of PD cases are sporadic, with only ten percent of PD cases having underlying genetic causes, the identification of PD-associated genes over the past two decades has greatly increased our understanding of key biochemical pathways implicated in the pathogenesis of the disease. Specifically, juvenile parkinsonism has been linked to autosomal mutations in the genes that encode the E3 Ub-ligase Parkin and the serine/threonine mitochondrial kinase PINK1 (Kitada et al., 1998; Valente et al., 2004). Studies in *Drosophila melanogaster* provided initial genetic evidence that suggested both proteins regulate mitochondrial function. PINK1^{-/-} and Parkin^{-/-} mutant flies displayed locomotor deficits, muscle degeneration, mitochondrial morphological abnormalities, and neuronal loss (Clark et al., 2006; Park et al., 2006; Yang et al., 2006). Rescue of the PINK1^{-/-} phenotype by Parkin overexpression, but not vice versa, suggested that PINK1 acts upstream of Parkin in a common mitochondrial quality control pathway (Clark et al., 2006; Park et al., 2006; Yang et al., 2006).

Mitochondrial dysfunction in PD

The first evidence linking mitochondrial dysfunction to PD arose with the observation that accidental exposure to 1-methyl-4-phenyl-1,2,3,6-tetrahydropyridine (MPTP) caused parkinsonism and DA neuron degeneration (Davis et al., 1979; Langston and Ballard, 1983). The conversion of MPTP by glial monoamine oxidase B (MAO-B) to MPP⁺ and its uptake into DA neurons via the DA reuptake pathway, was later found to inhibit complex I of the mitochondrial respiratory chain, which subsequently induces neuronal death (Javitch et al., 1985; Nicklas et al., 1985; Salach et al., 1984). More importantly, postmortem brains of PD patients were found to have anatomically specific complex I deficiency in the SN (Schapira et al., 1990). These findings have been recapitulated in animal models of PD, where administration of pesticides and herbicides that

selectively inhibit complex I, such as rotenone and paraquat, cause parkinsonism (Betarbet et al., 2000; Tanner et al., 2011). It has been proposed that the highly arborized axonal architecture of DA neurons in the SN contributes to their vulnerability and sensitivity toward mitochondrial dysfunction (Bolam and Pissadaki, 2012; Matsuda et al., 2009; Pissadaki and Bolam, 2013). Their high metabolic demands could result in the increased production of reactive oxygen species (ROS), damaging mitochondria and eventually resulting in neuronal cell death (Pacelli et al., 2015).

PINK1/Parkin mediated mitophagy

Parkin and PINK1 function in the same signaling pathway, mediating the degradation of damaged mitochondria by autophagy in a process termed mitophagy (Fig. 1). Under normal conditions, PINK1 is constitutively imported into the mitochondria and subsequently cleaved by proteases so that the C-terminal fragment can be degraded by the proteasome (Deas et al., 2011; Greene et al., 2012; Jin et al., 2010; Meissner et al., 2011; Yamano and Youle, 2013). Depolarization of mitochondria impedes mitochondrial import of PINK1 since this process requires an active proton gradient (Lazarou et al., 2012). Accumulated PINK1 on the outer surface of depolarized mitochondria phosphorylates Ub bound to mitochondrial proteins, which results in the recruitment of Parkin from the cytoplasm (Narendra et al., 2010; Tang et al., 2017; Zhou et al., 2008). Most notably, PINK1 phosphorylates Ub at its Ser65, along with Parkin at the homologous residue in its N-terminal Ub-like (Ubl) domain (Kazlauskaitė et al., 2014; Kondapalli et al., 2012; Koyano et al., 2014; Okatsu et al., 2015; Shiba-Fukushima et al., 2012). Phosphorylated Ub (pUb) binds Parkin, inducing allosteric changes that make the Ubl more accessible for phosphorylation by PINK1, which further enables Parkin to adopt an “active” conformation (Sauve et al., 2015). Parkin binds to the E2 Ub-conjugating enzyme and transfers the Ub onto its substrate via a thioester intermediate at its catalytic Cys431 (Wenzel et al., 2011). Ubiquitinated mitochondrial fusion

proteins Mfn1 and Mfn2 are then degraded by the proteasome, resulting in a reduction of mitochondrial fusion (Chan et al., 2011; Chen et al., 2003; Tanaka et al., 2010). Ub chains on substrates not targeted for proteasomal degradation can be phosphorylated by PINK1, triggering a feed-forward amplification of Parkin translocation to the mitochondria (Ordureau et al., 2014). Polyubiquitinated mitochondrial substrates also recruit autophagy adaptor proteins such as NBR1, p62, NDP52, and OPTN, which interact with LC3 to engulf the entire organelle into an autophagosome that will fuse with the lysosome for degradation (Heo et al., 2015; Lazarou et al., 2015).

Neuroprotective capacity of Parkin

Though the PINK1/Parkin mitophagy pathway has received considerable attention in the past decade, PINK1 and Parkin have been shown to be involved in another form of mitochondrial quality control by which mitochondria can remove damaged components through specialized structures called mitochondrial-derived vesicles (MDVs) that shuttle damaged, oxidized cargo from the mitochondria to the lysosome for degradation (McLelland et al., 2014; Soubannier et al., 2012). These findings suggest that the MDV and mitophagy pathways are activated depending on the level of mitochondrial damage, where mitochondria can selectively remove oxidized cargo through the formation of MDVs before damage is beyond repair and the turnover of the entire organelle is necessary. In this context, the current model of PD proposes that the loss of DA neurons is due to an accumulation of dysfunctional mitochondria as a result of defects in Parkin and PINK1 (Pickrell and Youle, 2015).

While the current model for Parkin activation is based on a cytosolic inactive form that becomes active at the mitochondria upon phosphorylation and recruitment by PINK1, there may be mechanisms that activate Parkin at non-mitochondrial localizations as Parkin is primarily

cytosolic and only becomes localized to mitochondria upon mitochondrial damage. Aside from its role in mitophagy, Parkin is involved in pro-survival pathways such as NF- κ B signaling. Parkin binds to the linear Ub assembly complex (LUBAC) and increases linear ubiquitination of NF- κ B essential modulator (NEMO), up-regulating NF- κ B target genes such as OPA1, which regulates cristae integrity and promotes mitochondrial fusion (Henn et al., 2007; Muller-Rischart et al., 2013). Another substrate of Parkin is Eps15, which upon ubiquitination delays epidermal growth factor receptor (EGFR) internalization, subsequently increasing Akt signalling and ultimately promoting neuronal survival (Fallon et al., 2006). Additionally, Parkin induces mitochondrial biogenesis by ubiquitinating the transcriptional repressor Parkin-interacting substrate (PARIS) subsequently targeting it for degradation by the proteasome (Shin et al., 2011; Stevens et al., 2015). Increased PARIS expression has been found in both sporadic and familial PD brains, which represses the expression of the master mitochondrial biogenesis gene, peroxisome proliferator-activated receptor gamma co-activator 1-alpha (PGC1 α) (Lee et al., 2017; Siddiqui et al., 2015).

Ubiquitination

Protein ubiquitination is a complex post-translational modification that fundamentally controls intracellular signalling events. Ub is a small protein (~8.5 kDa) that binds to substrates via its C-terminal glycine residue and can further form polyubiquitin chains via any of its seven lysine residues (Lys⁶, Lys¹¹, Lys²⁷, Lys²⁹, Lys³³, Lys⁴⁸, Lys⁶³). Different Ub linkages are implicated in distinct biological processes, which suggests that they are regulated and recognized independently. Lys⁴⁸-linked chains are the most abundant type of polyubiquitin chain formation in cells and have a well-established roll in signaling substrate degradation by the 26S proteasome (Thrower et al., 2000; Xu et al., 2009). The second most common polyubiquitin chain type, linked

via Lys⁶³, has various non-degradative signalling outputs that include DNA repair, endocytosis, and signal transduction (An et al., 2013; Chen and Sun, 2009; Gulia et al., 2017; Hofmann and Pickart, 1999).

The ubiquitination cascade is accomplished by the coordinated action of three enzymes: an E1 Ub-activating enzyme, an E2 Ub-conjugating enzyme, and an E3 Ub ligase. The E1 enzyme adenylates the carboxyl terminus of Ub in an ATP-dependent reaction and forms a covalent thioester linkage between its active cysteine and the C terminus of Ub (Ciechanover et al., 1981; Haas and Rose, 1982; Haas et al., 1982; Hershko et al., 1981). Ub is then transferred from the E1~Ub complex to the active cysteine of the E2 enzyme through a transthioesterification reaction (Hershko et al., 1983). An E3 will then interact with the E2~Ub complex to transfer the Ub from the active cysteine of the E2 to a substrate via an isopeptide bond between the C terminus of Ub and a lysine residue within the substrate (Hershko et al., 1983).

E3 Ligases

There are three families of E3 Ub ligases: RING (Really Interesting New Gene), HECT (Homologous to the E6-AP Carboxyl Terminus), and RBR (RING-between-RING). RING-type E3 ligases facilitate the direct transfer of Ub from the E2 to the substrate (Lorick et al., 1999). HECT ligases, however, form a Ub thioester intermediate via their active-site cysteine, from which Ub is transferred onto the substrate. RBR ligases use a RING/HECT hybrid mechanism, binding the E2 via their RING1 domain similarly to RING ligases, and forming a transient thioester intermediate reminiscent of HECT E3 ligases.

Parkin

Parkin is a member of the RBR family of E3 Ub ligases. It is comprised of a conserved N-terminal Ubl domain connected through a 60 amino acid (aa) linker to a zinc-binding domain called

RING0, followed by the catalytic RBR module common to other E3s. Structural studies have revealed that Parkin exists in an auto-inhibited conformation under basal conditions, with distinct interactions that keep it in an inactive state (Kumar et al., 2017; Sauve et al., 2015; Trempe et al., 2013). Firstly, the Ubl domain binds RING1, making Ser65 poorly accessible for phosphorylation by PINK1. Secondly, the repressor element of Parkin (REP), a linker region that separates the IBR and RING2 domain, binds to RING1, thereby blocking the E2 binding site and ultimately preventing transfer of Ub onto substrates. Finally, the catalytic Cys431 on the RING2 domain is physically occluded by RING0. These barriers must ultimately be overcome for Parkin to exhibit full E3 ligase activity. Site-directed mutagenesis studies have shown that disruption of these inhibitory interfaces results in faster translocation to depolarized mitochondria and more efficient ubiquitination of mitochondrial substrates (Sauve et al., 2015; Tang et al., 2017; Trempe et al., 2013).

Since its identification as a PD-associated gene, biological studies on Parkin have helped to elucidate the signaling pathways involved in the pathophysiology of the disease. The increased identification of Parkin substrates, both mitochondrial and non-mitochondrial, along with Parkin's wide neuroprotective capacity make Parkin a promising candidate for therapeutic strategies that could halt the progression of PD. However, not much is known about the conformational changes that occur during Parkin activation.

Förster resonance energy transfer (FRET)

The application of FRET has increasingly been used to study molecular interactions in both *in vivo* and *in vitro* systems. It is a process that describes the transfer of energy between a donor fluorophore and an acceptor fluorophore through non-radiative dipole-dipole coupling (Stryer, 1978). The efficiency of this energy transfer is inversely proportional to the sixth power of the

distance between both fluorophores, making FRET a useful molecular ruler (Stryer, 1978). FRET can detect interactions between proteins as well as provide information about protein conformation (Pollok and Heim, 1999; Truong and Ikura, 2001). While there are several potential FRET pairs, the most common one is CFP/YFP (cyan fluorescent protein/yellow fluorescent protein) (Miyawaki et al., 1997). FRET measurements can be affected by a number of factors, including photobleaching, orientation of the fluorophores, and quantum yield (reviewed in (Piston and Kremers, 2007), but the main limitation for the CFP/YFP FRET pair is the cross-talk in both the excitation and emission spectra of both fluorophores (Gordon et al., 1998). A modified FRET method developed by Xia and Liu (2001) gives consistent FRET values that are comparable among different cells with varying protein expression levels. For this reason, FRET is a suitable technique to study conformational changes during Parkin activation.

Aims

The overall aim of this thesis was to develop fluorescence-based assays to build on the insights provided by the crystal structure of Parkin and be used as screening tools to monitor Parkin activity.

1. Aim 1: To develop an assay that detects the transfer of Ub onto Parkin as a direct consequence of Parkin activation.

An *in vitro* auto-ubiquitination assay consisting of fluorescently-labelled Ub was designed to study Parkin activation. We hypothesize that higher fluorescence intensities will correlate with increasing amounts of fluorescently-labelled Ub bound to Parkin, which would suggest greater E3 ligase activity. Compounds that activate Parkin should result in higher fluorescence intensities observed.

2. Aim 2: To develop an assay capable of monitoring specific conformational changes that occur in Parkin upon activation.

Our lab has designed a structure-based FRET assay to investigate the structural changes during Parkin activation in cells using fluorescent probes. We have previously shown that point mutations designed to depress Parkin's auto-inhibited conformation resulted in FRET efficiency changes. These mutations correlated with an increased E3 ligase activity as well as an accelerated rate of recruitment to the mitochondria (Tang et al., 2017). We hypothesize that compounds capable of activating Parkin will result in FRET efficiency changes.

3. Aim 3: To develop an assay capable of discriminating between direct and indirect Parkin activation.

A modified *in vitro* FRET assay can be used complementary to the cell-based FRET assay to validate small-molecule activators of Parkin. We hypothesize that compounds capable of activating Parkin through direct binding should result in FRET efficiency changes, whereas compounds that indirectly activate Parkin through other cellular pathways should display no changes in FRET efficiency.

Methods

Cloning of FRET reporter constructs

H. sapiens Parkin tagged with enhanced green fluorescent protein (eGFP-HsParkin) was amplified using PCR with primers containing HindIII and BamHI. The amplified product was cut with HindIII and BamHI and inserted into pCDNA3. mVenus-N1 (Addgene plasmid #27793) was inserted at various sites within Parkin by PCR and then further amplified with primers containing BglII and HindIII. The amplified product was cut with BglII and HindIII and inserted into mCerulean-C1 (Addgene plasmid #27796). C17V (Addgene plasmid #26395), a construct that

contains Cerulean attached to Venus via a 17 aa linker, was used as a positive control. The mVenus-N1, the mCerulean-C1, and the C17V constructs were gifts from Dr. Steven Vogel.

Cloning and production of purified recombinant proteins

Rattus norvegicus Parkin (*RnParkin*) DNA was codon-optimized for *E. coli* expression (DNA Express Inc.) and subcloned into pGEX-6P-1 using BamHI and XhoI restriction enzymes to generate glutathione S-transferase (GST)-*RnParkin*. Single-point mutations were introduced using PCR site-directed mutagenesis according to the manufacturer's protocol (Agilent Technologies) to generate GST-*RnParkin* W403A and GST-*RnParkin* C431A. Parkin variants were transformed in BL21 (DE3) *E. coli* cells (NEB) and pre-cultured overnight in 20 ml of lysogeny broth (LB) medium supplemented with 100 $\mu\text{g ml}^{-1}$ Ampicillin at 37 °C and 200 rpm. The overnight cultures were then transferred to 2 L of fresh medium and incubated at 37 °C and 200 rpm until an optical density at 600 nm of ~ 0.6 was obtained. Protein expression was induced with 25 μM isopropyl- β -D-thiogalactoside (IPTG) and 25 μM Zn_2SO_4 at 4 °C and 200 rpm for 18 h. *E. coli* were harvested by centrifugation at 35000 rpm and resuspended in 40 ml of tris-buffered saline (TBS) (50 mM Tris-HCl, 120 mM NaCl, 1 mM DTT, pH 7.5) containing 0.5% Tween-20 and protease inhibitors. The cell suspension was then frozen at -80 °C, thawed, and sonicated before ultracentrifugation at 18000 rpm. The clear lysate was incubated on GSH-sepharose beads slurry (GE Healthcare) for 1 h at 4 °C and proteins eluted with 20 mM GSH. The purified Parkin variants were applied to a Superdex 200 16/600 column (GE Healthcare) in TBS buffer. GST fused *T. castaneum* PINK1 (GST-*TcPINK*) was purified in a similar manner to Parkin but cleaved by 3C before size-exclusion chromatography in TBS buffer, pH 8. *HsParkin* FRET reporters were cloned from mCerulean-C1 vectors into pGEX-6P-1 by Gibson Assembly (NEB), purified as described above, cleaved by 3C, and applied to a Superdex 200 10/300 column (GE Healthcare). Protein

concentrations were determined by ultraviolet absorption at 280 nm using the theoretical extinction coefficients.

Ub labelling

H. sapiens Ub (Boston Biochem) was labelled with Alexa Fluor 594 NHS Ester (Thermo Fisher) at a molar ratio of 20:1 and pH 7 in a reaction volume of 100 μ l. Labelling was performed at room temperature for 10 min. The reaction was stopped with 10 μ l of 1M Tris, pH 8.8 and buffer exchanged using Amicon Ultra Centrifugal Filters (Millipore Sigma). Mass spectrometry was then performed to determine labelling efficiency.

In vitro phosphorylation of Ub by TcPINK1

Ub phosphorylation was performed at 30 °C for 1 h with 0.1 mg ml⁻¹ TcPINK1 and 25 μ M Ub in 50 mM Tris/HCl, pH 7.5, 120 mM NaCl, 1 mM DTT, 1 mM ATP, 5 mM MgSO₄ in a reaction volume of 100 μ l. The reaction was separated on a Superdex 75 10/300 column (GE Healthcare) in HEPES buffer, pH 7. Purified pUb was analyzed by SDS-PAGE on 10% Tris-glycine gels containing 20 μ M Phos-tag (Wako Laboratory Chemicals) and 40 μ M MnCl₂ and stained with Coomassie.

Auto-ubiquitination assays

Ubiquitination assays were performed at 37 °C in the presence of 50 mM Tris/HCl, pH 7.5, 120 mM NaCl, 1 mM DTT, 4 mM ATP, 10 mM MgCl₂, 50 nM E1 (Boston Biochem), 2 μ M Ubch7, 2 μ M RnParkin, with or without TcPINK1, and 3 μ M pUb. Reactions were stopped with 3X sample buffer containing 100 mM DTT and analyzed by SDS-PAGE on 8% Tris-glycine gels. Proteins were transferred to nitrocellulose. Membranes were blocked with 5% milk in phosphate-buffered saline (PBS) containing 0.1% Tween 20 (PBS-T) and incubated with mouse anti-Parkin (1:40,000, mAb PRK8, Santa Cruz Biotechnology), mouse anti-Ub (1:2,000, mAb P4D1, Santa

Cruz Biotechnology), or rabbit anti-GST (1:2,000) diluted in PBS-T with 3% Bovine Serum Albumin (BSA). Membranes were washed with PBS-T and incubated with HRP-coupled goat anti-mouse or anti-rabbit IgG antibodies (1:5,000, Jackson Laboratories). Detection was performed with Pierce ECL Western Blotting Substrate (Thermo Fisher).

Pierce glutathione (GSH)-coated, black, 96-well plates (Thermo Fisher) were rinsed three times with 200 μ l of wash buffer (TBS buffer containing 0.05% Tween). 40 μ g of GST-*Rn*Parkin variants were added to each well, incubated at 4 °C for 15 min, and rinsed twice with 200 μ l of wash buffer. The auto-ubiquitination assay was carried out for 2 h with the conditions described above. The plate was then rinsed twice with 200 μ l of wash buffer and fluorescence intensity (Ex/Em 590/617 nm) was measured using a TECAN infinite M200 fluorescence plate reader. 3X sample buffer containing 100 mM DTT was then added to each well and samples were analyzed by SDS-PAGE on 8% Tris-glycine gels as described above.

Cell culture

Human osteosarcoma U2OS cells were transfected with either *Hs*Parkin FRET constructs, or an ecdysone-inducible mitochondrially-targeted mKeima (mt-Keima) (a gift from A. Miyawaki, Laboratory for Cell Function and Dynamics, Brain Science Institute, RIKEN, Japan) using jetPRIME (Polyplus), followed by selection with G418 for 1 week and sorted using flow cytometry. Cells were maintained in DMEM supplemented with 10% fetal bovine serum (FBS), 4 mM L-glutamine and 0.1 % Penicillin/Streptomycin, and kept in a 37 °C incubator with 5 % CO₂.

FRET analysis

*Hs*Parkin FRET reporters were transfected into HeLa cells for 24 h prior to FRET measurements. Images were acquired using a Zeiss AxioObserver.Z1 inverted fluorescent microscope with FRET filters (47 HE Cyan, 46 HE Yellow, and 48 CFP-YFP-FRET) and a 63x

oil immersion objective. FRET efficiencies were determined by the Zeiss AxioVision software using the Xia method (Xia and Liu, 2001).

U2OS cells were seeded on 96 well black, clear bottom plates at a density of 10,000 cells/well. Cells were transfected with *HsParkin* FRET reporters and fluorescence intensities for CFP (Ex/Em 435/485 nm), YFP (Ex/Em 495/545 nm), and FRET (Ex/Em 435/545 nm) were measured using a TECAN infinite M200 fluorescence plate reader. FRET efficiencies were calculated using the Xia formula.

For high-content screening (HCS), U2OS cells stably expressing *HsParkin* FRET-380 variants were imaged on either an Opera Phenix HCS System (Perkin Elmer) with a 20x air objective and spinning disk confocal using the FRET module, or on a CellInsight CX7 HCS Platform (Thermo Fisher) with a 10x air objective, CFP excitation 386/23, CFP emission 482/25, YFP excitation 485/20, and YFP emission 542/27.

For the *in vitro* FRET assay, 2 μ g of recombinant *HsParkin* FRET reporter was incubated in 50 mM Tris/HCl, pH 7.5, 120 mM NaCl, 1 mM DTT, 1 mM ATP, 10 mM MgCl₂, with or without *TcPINK1*, and 3 μ M pUb in a reaction volume of 100 μ l. *In vitro* FRET measurements were performed using a TECAN infinite M200 fluorescence plate reader with the exact settings already mentioned above.

For statistical analyses, one-way ANOVA followed by a Dunnett's test was performed using Graph Pad Prism 6 (la Jolla, CA). Data was obtained from two independent experiments and findings were considered significant as follows: **** $P < 0.0001$; n.s., nonsignificant.

The Z-factor for the cell-based FRET assay was estimated from two independent experiments for each HCS system. Z' values between 0.5 and 1 were interpreted as an "excellent assay" and presumed to have a large enough response to warrant further attention.

Parkin recruitment assay

U2OS cells stably expressing *HsParkin* FRET constructs were seeded on a 35 mm Glass Bottom Microwell Dish (MatTek Corporation) at a density of 300,000 cells/dish and treated with 20 μ M carbonyl cyanide *m*-chlorophenyl hydrazone (CCCP). Images were acquired every 5 min for a total of 90 min using the 46 HE Yellow filter on the Zeiss AxioObserver.Z1 inverted fluorescent microscope. Parkin recruitment was calculated as a percentage of cells that showed the appearance of YFP fluorescence puncta on the mitochondria (Tang et al., 2017).

Mitophagy assay

U2OS cells stably expressing mtKeima were induced with 10 μ M ponasterone A, transfected with *HsParkin* FRET constructs for 18 h, and treated with 20 μ M CCCP for 4 h. Cells were trypsinized, washed, and resuspended in PBS for fluorescence-activated cell sorting (FACS)-based analysis on a LSR Fortessa (BD Bioscience). Data was analyzed using FlowJo v10.1 (Tree Star) and mitophagy was quantified as the ratio of cells that shifted excitation at 405 nm, pH 7, to 561 nm, pH 4.

Results

Auto-ubiquitination assay

The crystal structure of Parkin revealed distinct interactions that result in an auto-inhibited conformation under basal conditions; however, disruption of these interfaces by site-directed mutagenesis results in faster translocation to depolarized mitochondria, more efficient ubiquitination of mitochondrial substrates and increased Parkin auto-ubiquitination (Sauve et al., 2015; Tang et al., 2017; Trempe et al., 2013). We designed an unbiased Parkin auto-ubiquitination assay consisting of GST-*Rn*Parkin and fluorescently-labelled Ub that could detect the transfer of Ub onto Parkin as a direct consequence of Parkin activation (Fig. 2a).

Labelling Ub

Our labelling technique of choice for Ub in the auto-ubiquitination assay was the amine-reactive probe Alexa Fluor. These fluorescent dyes are bright and relatively small (~1kDa) in comparison to fluorescent proteins (~30kDa). The succinimidyl (NHS) ester of Alexa Fluor allows for conjugation of the dye to amine-containing molecules. Since Ub binds to substrates via its C-terminus and forms polyubiquitin chains via its seven side lysine residues, we sought to selectively label the N-terminus (Komander, 2009). While the NHS ester Alexa Fluor dyes usually label all amino groups, selective labelling of the terminal amine is possible at neutral pH as the pKa of the terminal amine is lower than that of the ϵ amino (Grimsley et al., 2009). Since many small molecules found in libraries used for screening tend to interfere in the blue-green spectral region, we chose to label Ub with a red-shifted dye to decrease the likelihood of interference from the compound library (Simeonov and Davis, 2004). Several Alexa Fluor dyes were tested at varying molar ratios, time points, and pH (Supplementary Fig. 1-5).

Labelled Ub can form polyubiquitin chains

Our Alexa Fluor dye of choice was Alexa 594, and mass spectrometry showed Ub was mostly labelled with only one molecule of Alexa 594, meaning that most side lysine residues were still available to form polyubiquitin chains (Fig. 2b); however, tandem mass spectrometry showed a diverse population of labelled Ub, with Lys⁴⁸ and Lys⁶³ being the residues that were predominantly labelled (Supplementary Fig. 6). Since we were unable to selectively label the N-terminus of Ub, we tested the Ub labelled with Alexa 594 (Ub⁵⁹⁴) in an *in vitro* auto-ubiquitination reaction for its ability to form polyubiquitin chains on Parkin. Addition of pUb or PINK1 to the reaction resulted in higher order polyubiquitin chains, while addition of both pUb and PINK1 showed the highest order of polyubiquitin chains (Fig. 2c). Additionally, the catalytically inactive

mutant C431A had no ligase activity, whereas the hyperactive mutant W403A showed higher E3 ligase activity than WT for all conditions (Fig. 2c).

Auto-ubiquitination assay on GSH-coated plates

We then tested the binding capacity and the binding efficiency of GSH-coated, black, 96-well plates (Thermo Fisher) and were able to bind ~100 ng of GST-*Rn*Parkin per well (Supplementary Fig. 7a, b). Auto-ubiquitination reactions were then performed, but no fluorescence was detected after the plate had been rinsed. Samples were analyzed by immunoblotting and polyubiquitination was observed, suggesting that the fluorescence intensity from the Ub⁵⁹⁴ that was bound to Parkin was insufficient for detection on the plate reader (Supplementary Fig. 7c). Therefore, this approach was no longer pursued.

Monitoring conformational changes within Parkin

The second assay utilizes FRET to detect conformational changes within Parkin. We designed a series of FRET reporter constructs with the donor cyan fluorescence protein (CFP) Cerulean at the N-terminus of Parkin, and the acceptor yellow fluorescent protein (YFP) Venus at various locations within Parkin (Fig. 3a). Under basal conditions, Parkin is in a ‘closed’ conformation, and therefore has a high FRET efficiency as both fluorescent proteins are within close enough proximity. Upon activation, Parkin undergoes conformational changes that render these fluorescent proteins further away from each other, lowering their FRET efficiency (Fig. 3b).

Kinetics and activity of FRET reporters

To ensure that the fluorescent protein inserted into the linkers that connect different domains in Parkin did not interfere with its function, we first tested all constructs in a mitochondrial recruitment assay. Insertion of YFP at positions 81 (after Ubl), 129 (linker between Ubl and RING0), and 380 (linker between IBR and REP) had similar kinetics to Parkin tagged

with YFP at the N-terminus, while insertion of YFP at positions 140 (before RING0), 356 (loop within RBR), and 466 (C-terminus) delayed Parkin recruitment to the mitochondria following addition of the protonophore uncoupling agent CCCP; therefore, these constructs were not further analyzed (Fig. 4a). We then tested the FRET reporters with unaffected kinetics in a FACS-based mitophagy assay. All constructs were able to efficiently induce mitophagy upon mitochondrial depolarization with CCCP (Fig. 4b, c).

Activating mutations result in decreased FRET efficiencies

HeLa cells were transfected with the FRET reporters and FRET microscopy measurements were performed. Basal FRET efficiencies were higher for constructs with shorter predicted distances between their fluorophores (Fig. 5a). The FRET-380 reporter, with its high basal FRET efficiency, was chosen as the most suitable for monitoring conformational changes associated with Parkin activation. The phosphomimetic S65E mutation as well as mutations predicted to disrupt the RING0:RING2 interface (F146A), the UBL:RING1 interface (N273K), and the REP:RING1 interface (W403A), resulted in decreased FRET efficiencies, suggesting an “open” more active conformation (Fig. 5b, c).

Testing FRET reporters for HCS

U2OS cells transiently transfected with *HsParkin* FRET reporters were tested on a fluorescence plate reader (TECAN). We used the C17V construct as a positive control for our assay. The C17V construct, containing Cerulean attached via a 17 aa linker to Venus, is a good indicator of FRET efficiency due to the close proximity of both fluorescent proteins (Koushik et al., 2006). The values obtained from the plate reader followed the same trend that was observed with the transiently transfected HeLa cells on the fluorescence microscope, with FRET-380 displaying the highest FRET efficiency and FRET-129 having the lowest FRET efficiency (Fig.

6a). U2OS cells stably expressing FRET-380 variants were tested on two high content microscopes: Opera Phenix HCS System (Perkin Elmer) and CellInsight CX7 HCS Platform (Thermo Fisher). The change in FRET efficiency between FRET-380 WT and FRET-380 W403A observed was 35% on the Opera Phenix and 20% on the CX7. More importantly, the Z' obtained was 0.62 on the Opera Phenix and 0.78 on the CX7 (Fig. 6b). The Z factor is a statistical measure used in HCS to judge whether a response in a certain assay is large enough to warrant further attention (Zhang et al., 1999). Assays with Z' values between 0.5 and 1 are seen as good assays. Based on this criterion, our cell-based FRET assay appears to be a promising screen to identify small-molecule activators of Parkin.

In vitro FRET assay

Recombinant *HsParkin* FRET reporters were purified and confirmed to be stable and susceptible to activation by phosphorylation by PINK1 in an *in vitro* auto-ubiquitination assay (Fig. 7a). Moreover, addition of known Parkin activators such as pUb or PINK1 decreased FRET efficiency in our recombinant FRET-380 protein (Fig. 7b). The goal for this modified *in vitro* FRET assay is to further validate hits from the cell-based FRET assay. FRET changes should be observed for compounds that bind directly to Parkin, while no FRET changes should be observed for compounds that activate Parkin indirectly.

Discussion

Loss of function mutations in *Parkin* that decrease or abolish its E3 Ub ligase activity have been linked to inherited forms of PD. Parkin exists basally in an auto-inhibited form that requires several activation steps and conformational rearrangements in order to achieve full E3 ligase activity. We have developed three fluorescence-based assays that can monitor Parkin activity. The first assay detects the transfer of Ub onto Parkin as a direct consequence of Parkin activation. Since

commercially available Ub N-Terminal Fluorescein (Boston Biochem) is not cost-effective for an HCS, we attempted to selectively label Ub at the N-terminus using Alexa 594. Our labelling technique generated a diverse population of unlabelled and labelled Ub (Fig. 2b). Parkin has been shown to form polyubiquitin chains primarily composed of canonical Lys⁴⁸ and Lys⁶³ linkage chains, as well as noncanonical Lys⁶ and Lys¹¹ linkage chains, with little evidence of Met¹, Lys²⁷, Lys²⁹, or Lys³³ linkage chains (Durcan et al., 2014; Ordureau et al., 2014). The population of our Ub⁵⁹⁴ is mostly labelled on Lys⁴⁸ and Lys⁶³, which are the two lysine residues that Parkin preferentially uses for polyubiquitin chain assembly (Supplementary Fig. 6). Unlabelled Ub in our sample is likely the population that is mostly binding to Parkin, which could explain the absence of fluorescence observed using the plate reader. Additionally, the GSH-coated plates used in our assay can only bind a small amount of GST-*Rn*Parkin (~100 ng), which further decreases the fluorescence that can be detected by the plate reader. While we cannot increase the amount of GST-*Rn*Parkin that binds to the plates, attempts can be made to selectively label the N-terminus of Ub using a sortase-mediated reaction to yield a more homogeneous population of labelled Ub (Theile et al., 2013). The design for the auto-ubiquitination assay as a primary screen for small-molecules that could activate Parkin appeared promising as we are able to purify large amounts of GST-*Rn*Parkin (Supplementary Fig. 8a); however, unless we can increase the amount of fluorescently-labelled Ub bound to the plates, it is unlikely that this assay will be used as a screen.

The second assay is a cell-based FRET assay that monitors specific conformational changes that occur in Parkin during activation. We showed that our *Hs*Parkin FRET reporters are able to detect conformational changes within Parkin (Fig. 5) without interfering with its recruitment kinetics (Fig. 4a) or its ability to perform mitophagy (Fig. 4b, c). Our U2OS cells stably expressing *Hs*Parkin FRET-380 variants have been tested on HCS systems, yielding a Z'

above 0.5, which suggests our assay would be a useful high-throughput screen. The next step for our cell-based FRET assay is to test a Library of Pharmacologically Active Compounds. Top hits from the cell-based FRET assay can be further validated with our modified *in vitro* FRET assay to discriminate between compounds that activate Parkin indirectly (ie. by inducing mitochondrial depolarization) versus those that directly bind Parkin. We have shown that our recombinant *HsParkin* FRET reporters have ligase activity (Fig. 7a) and that changes in FRET efficiency can be detected with FRET-380 upon addition of known Parkin activators such as pUb and PINK1 (Fig. 7b).

E3 Ub ligases have gained increased attention as targets for drug discovery due to their specific homeostatic regulation of various biological processes. While several screens have been developed to identify regulators of Parkin, these screens often depend on Parkin localizing to the mitochondria (Hasson et al., 2013; Morrison et al., 2011; Potting et al., 2018; Villace et al., 2017). Even the current model for Parkin activation is based on the concept that a cytosolic, inactive form of Parkin is recruited to the mitochondria and phosphorylated by PINK1 upon mitochondrial depolarization (Narendra et al., 2008; Narendra et al., 2010; Tang et al., 2017). However, Parkin is mostly cytosolic and is involved in several pathways outside the mitochondria, meaning that Parkin must have a different mechanism for cytosolic activation (Fallon et al., 2006; Henn et al., 2007; Shin et al., 2011). Our FRET assays do not depend on mitochondrial localization and can therefore allow for the characterization of endogenous activators of Parkin. Based on structural studies, several sites of inhibition contribute to the basally, auto-inhibited, cytosolic conformation of Parkin. We have shown that disruption of these interfaces through site-directed mutagenesis can render Parkin hyperactive. Specifically, disruption of the REP:RING1 interaction allows for E2

binding. The ultimate goal for our assays is to find a small-molecule that will activate Parkin through conformational changes that will disrupt the REP:RING1 interface.

While serendipity played an important role in drug discovery in the past, drug design presently is challenged by the identification of potential drug targets in key biological pathways. Protein structures solved by x-ray crystallography, in particular, allow for the generation of rationally designed libraries of compounds. Parkin mutations designed to disrupt sites of inhibition, for example, propose a basis for potential drug scaffold identification. PD patients with *Parkin* mutations would benefit from compounds designed to bind specific domains in Parkin that could rescue those mutations, while sporadic PD patients could benefit from an overall increase in Parkin activity as downstream activation of pro-survival pathways could halt or delay DA cell death. Our FRET assays serve as an unbiased biological pipeline by which these compounds can be tested through automated high-throughput screening, increasing the success rate of finding suitable drug candidates. Identification of compounds can then be further validated through activity-based assays such as Parkin auto-ubiquitination, ubiquitination of mitochondrial substrates, Parkin recruitment, and mitophagy.

Conclusion

PD is the second most common neurodegenerative disease, wherein patients exhibit both motor and non-motor symptoms. While there is no current cure for the disease, medications, surgery, and physical treatment can help manage symptoms. The discovery of PD-linked genes has greatly increased our understanding of the biological mechanisms involved in the pathophysiology of the disease. *Parkin* was identified 20 years ago as a PD-associated gene. Since then, a number of studies have investigated its structure, its activation mechanism, and its activity as an E3 Ub ligase in various pathways. Since Parkin exhibits wide neuroprotective activity under

various stress conditions, it is an attractive target for drug discovery as it is hypothesized that increasing Parkin activity could be a therapeutic strategy. The development of assays that can monitor Parkin activity can guide the discovery of regulators or small-molecule activators that could be further developed into new drugs for the treatment of PD. Innovative partnerships between the scientific community and the pharmaceutical industry are essential for taking research from “bench-to-bedside” and accelerating the development of ground-breaking therapies.

References

- An, L., W. Jia, Y. Yu, N. Zou, L. Liang, Y. Zhao, Y. Fan, J. Cheng, Z. Shi, G. Xu, G. Li, J. Yang, and H. Zhang. 2013. Lys63-linked polyubiquitination of BRAF at lysine 578 is required for BRAF-mediated signaling. *Sci Rep.* 3:2344.
- Betarbet, R., T.B. Sherer, G. MacKenzie, M. Garcia-Osuna, A.V. Panov, and J.T. Greenamyre. 2000. Chronic systemic pesticide exposure reproduces features of Parkinson's disease. *Nat Neurosci.* 3:1301-1306.
- Bolam, J.P., and E.K. Pissadaki. 2012. Living on the edge with too many mouths to feed: why dopamine neurons die. *Mov Disord.* 27:1478-1483.
- Chan, N.C., A.M. Salazar, A.H. Pham, M.J. Sweredoski, N.J. Kolawa, R.L. Graham, S. Hess, and D.C. Chan. 2011. Broad activation of the ubiquitin-proteasome system by Parkin is critical for mitophagy. *Hum Mol Genet.* 20:1726-1737.
- Chen, H., S.A. Detmer, A.J. Ewald, E.E. Griffin, S.E. Fraser, and D.C. Chan. 2003. Mitofusins Mfn1 and Mfn2 coordinately regulate mitochondrial fusion and are essential for embryonic development. *J Cell Biol.* 160:189-200.
- Chen, Z.J., and L.J. Sun. 2009. Nonproteolytic functions of ubiquitin in cell signaling. *Mol Cell.* 33:275-286.
- Ciechanover, A., H. Heller, R. Katz-Etzion, and A. Hershko. 1981. Activation of the heat-stable polypeptide of the ATP-dependent proteolytic system. *Proc Natl Acad Sci U S A.* 78:761-765.
- Clark, I.E., M.W. Dodson, C. Jiang, J.H. Cao, J.R. Huh, J.H. Seol, S.J. Yoo, B.A. Hay, and M. Guo. 2006. Drosophila pink1 is required for mitochondrial function and interacts genetically with parkin. *Nature.* 441:1162-1166.
- Davis, G.C., A.C. Williams, S.P. Markey, M.H. Ebert, E.D. Caine, C.M. Reichert, and I.J. Kopin. 1979. Chronic Parkinsonism secondary to intravenous injection of meperidine analogues. *Psychiatry Res.* 1:249-254.
- de Rijk, M.C., L.J. Launer, K. Berger, M.M. Breteler, J.F. Dartigues, M. Baldereschi, L. Fratiglioni, A. Lobo, J. Martinez-Lage, C. Trenkwalder, and A. Hofman. 2000. Prevalence of Parkinson's disease in Europe: A collaborative study of population-based cohorts. Neurologic Diseases in the Elderly Research Group. *Neurology.* 54:S21-23.
- Deas, E., H. Plun-Favreau, S. Gandhi, H. Desmond, S. Kjaer, S.H. Loh, A.E. Renton, R.J. Harvey, A.J. Whitworth, L.M. Martins, A.Y. Abramov, and N.W. Wood. 2011. PINK1 cleavage at position A103 by the mitochondrial protease PARL. *Hum Mol Genet.* 20:867-879.
- Durcan, T.M., M.Y. Tang, J.R. Perusse, E.A. Dashti, M.A. Aguilera, G.L. McLelland, P. Gros, T.A. Shaler, D. Faubert, B. Coulombe, and E.A. Fon. 2014. USP8 regulates mitophagy by removing K6-linked ubiquitin conjugates from parkin. *EMBO J.* 33:2473-2491.
- Fallon, L., C.M. Belanger, A.T. Corera, M. Kontogianna, E. Regan-Klapisz, F. Moreau, J. Voortman, M. Haber, G. Rouleau, T. Thorarinsdottir, A. Brice, P.M. van Bergen En Henegouwen, and E.A. Fon. 2006. A regulated interaction with the UIM protein Eps15 implicates parkin in EGF receptor trafficking and PI(3)K-Akt signalling. *Nat Cell Biol.* 8:834-842.
- Gordon, G.W., G. Berry, X.H. Liang, B. Levine, and B. Herman. 1998. Quantitative fluorescence resonance energy transfer measurements using fluorescence microscopy. *Biophys J.* 74:2702-2713.

- Greene, A.W., K. Grenier, M.A. Aguilera, S. Muise, R. Farazifard, M.E. Haque, H.M. McBride, D.S. Park, and E.A. Fon. 2012. Mitochondrial processing peptidase regulates PINK1 processing, import and Parkin recruitment. *EMBO Rep.* 13:378-385.
- Grimsley, G.R., J.M. Scholtz, and C.N. Pace. 2009. A summary of the measured pK values of the ionizable groups in folded proteins. *Protein Sci.* 18:247-251.
- Gulia, R., R. Sharma, and S. Bhattacharyya. 2017. A Critical Role for Ubiquitination in the Endocytosis of Glutamate Receptors. *J Biol Chem.* 292:1426-1437.
- Haas, A.L., and I.A. Rose. 1982. The mechanism of ubiquitin activating enzyme. A kinetic and equilibrium analysis. *J Biol Chem.* 257:10329-10337.
- Haas, A.L., J.V. Warms, A. Hershko, and I.A. Rose. 1982. Ubiquitin-activating enzyme. Mechanism and role in protein-ubiquitin conjugation. *J Biol Chem.* 257:2543-2548.
- Hasson, S.A., L.A. Kane, K. Yamano, C.H. Huang, D.A. Sliter, E. Buehler, C. Wang, S.M. Heman-Ackah, T. Hessa, R. Guha, S.E. Martin, and R.J. Youle. 2013. High-content genome-wide RNAi screens identify regulators of parkin upstream of mitophagy. *Nature.* 504:291-295.
- Henn, I.H., L. Bouman, J.S. Schlehe, A. Schlierf, J.E. Schramm, E. Wegener, K. Nakaso, C. Culmsee, B. Berninger, D. Krappmann, J. Tatzelt, and K.F. Winklhofer. 2007. Parkin mediates neuroprotection through activation of IkappaB kinase/nuclear factor-kappaB signaling. *J Neurosci.* 27:1868-1878.
- Heo, J.M., A. Ordureau, J.A. Paulo, J. Rinehart, and J.W. Harper. 2015. The PINK1-PARKIN Mitochondrial Ubiquitylation Pathway Drives a Program of OPTN/NDP52 Recruitment and TBK1 Activation to Promote Mitophagy. *Mol Cell.* 60:7-20.
- Hershko, A., A. Ciechanover, and I.A. Rose. 1981. Identification of the active amino acid residue of the polypeptide of ATP-dependent protein breakdown. *J Biol Chem.* 256:1525-1528.
- Hershko, A., H. Heller, S. Elias, and A. Ciechanover. 1983. Components of ubiquitin-protein ligase system. Resolution, affinity purification, and role in protein breakdown. *J Biol Chem.* 258:8206-8214.
- Hofmann, R.M., and C.M. Pickart. 1999. Noncanonical MMS2-encoded ubiquitin-conjugating enzyme functions in assembly of novel polyubiquitin chains for DNA repair. *Cell.* 96:645-653.
- Javitch, J.A., R.J. D'Amato, S.M. Strittmatter, and S.H. Snyder. 1985. Parkinsonism-inducing neurotoxin, N-methyl-4-phenyl-1,2,3,6 -tetrahydropyridine: uptake of the metabolite N-methyl-4-phenylpyridine by dopamine neurons explains selective toxicity. *Proc Natl Acad Sci U S A.* 82:2173-2177.
- Jin, S.M., M. Lazarou, C. Wang, L.A. Kane, D.P. Narendra, and R.J. Youle. 2010. Mitochondrial membrane potential regulates PINK1 import and proteolytic destabilization by PARL. *J Cell Biol.* 191:933-942.
- Kazlauskaitė, A., C. Kondapalli, R. Gourlay, D.G. Campbell, M.S. Ritorto, K. Hofmann, D.R. Alessi, A. Knebel, M. Trost, and M.M. Muqit. 2014. Parkin is activated by PINK1-dependent phosphorylation of ubiquitin at Ser65. *Biochem J.* 460:127-139.
- Kitada, T., S. Asakawa, N. Hattori, H. Matsumine, Y. Yamamura, S. Minoshima, M. Yokochi, Y. Mizuno, and N. Shimizu. 1998. Mutations in the parkin gene cause autosomal recessive juvenile parkinsonism. *Nature.* 392:605-608.
- Komander, D. 2009. The emerging complexity of protein ubiquitination. *Biochem Soc Trans.* 37:937-953.

- Kondapalli, C., A. Kazlauskaitė, N. Zhang, H.I. Woodroof, D.G. Campbell, R. Gourlay, L. Burchell, H. Walden, T.J. Macartney, M. Deak, A. Knebel, D.R. Alessi, and M.M. Muqit. 2012. PINK1 is activated by mitochondrial membrane potential depolarization and stimulates Parkin E3 ligase activity by phosphorylating Serine 65. *Open Biol.* 2:120080.
- Koushik, S.V., H. Chen, C. Thaler, H.L. Puhl, 3rd, and S.S. Vogel. 2006. Cerulean, Venus, and VenusY67C FRET reference standards. *Biophys J.* 91:L99-L101.
- Koyano, F., K. Okatsu, H. Kosako, Y. Tamura, E. Go, M. Kimura, Y. Kimura, H. Tsuchiya, H. Yoshihara, T. Hirokawa, T. Endo, E.A. Fon, J.F. Trempe, Y. Saeki, K. Tanaka, and N. Matsuda. 2014. Ubiquitin is phosphorylated by PINK1 to activate parkin. *Nature.* 510:162-166.
- Kumar, A., V.K. Chaugule, T.E.C. Condos, K.R. Barber, C. Johnson, R. Toth, R. Sundaramoorthy, A. Knebel, G.S. Shaw, and H. Walden. 2017. Parkin-phosphoubiquitin complex reveals cryptic ubiquitin-binding site required for RBR ligase activity. *Nat Struct Mol Biol.*
- Lang, A.E., and A.M. Lozano. 1998a. Parkinson's disease. First of two parts. *N Engl J Med.* 339:1044-1053.
- Lang, A.E., and A.M. Lozano. 1998b. Parkinson's disease. Second of two parts. *N Engl J Med.* 339:1130-1143.
- Langston, J.W., and P.A. Ballard, Jr. 1983. Parkinson's disease in a chemist working with 1-methyl-4-phenyl-1,2,5,6-tetrahydropyridine. *N Engl J Med.* 309:310.
- Lazarou, M., S.M. Jin, L.A. Kane, and R.J. Youle. 2012. Role of PINK1 binding to the TOM complex and alternate intracellular membranes in recruitment and activation of the E3 ligase Parkin. *Dev Cell.* 22:320-333.
- Lazarou, M., D.A. Sliter, L.A. Kane, S.A. Sarraf, C. Wang, J.L. Burman, D.P. Sideris, A.I. Fogel, and R.J. Youle. 2015. The ubiquitin kinase PINK1 recruits autophagy receptors to induce mitophagy. *Nature.* 524:309-314.
- Lee, Y., D.A. Stevens, S.U. Kang, H. Jiang, Y.I. Lee, H.S. Ko, L.A. Scarffe, G.E. Umanah, H. Kang, S. Ham, T.I. Kam, K. Allen, S. Brahmachari, J.W. Kim, S. Neifert, S.P. Yun, F.C. Fiesel, W. Springer, V.L. Dawson, J.H. Shin, and T.M. Dawson. 2017. PINK1 Primes Parkin-Mediated Ubiquitination of PARIS in Dopaminergic Neuronal Survival. *Cell Rep.* 18:918-932.
- Lorick, K.L., J.P. Jensen, S. Fang, A.M. Ong, S. Hatakeyama, and A.M. Weissman. 1999. RING fingers mediate ubiquitin-conjugating enzyme (E2)-dependent ubiquitination. *Proc Natl Acad Sci U S A.* 96:11364-11369.
- Matsuda, W., T. Furuta, K.C. Nakamura, H. Hioki, F. Fujiyama, R. Arai, and T. Kaneko. 2009. Single nigrostriatal dopaminergic neurons form widely spread and highly dense axonal arborizations in the neostriatum. *J Neurosci.* 29:444-453.
- McLelland, G.L., V. Soubannier, C.X. Chen, H.M. McBride, and E.A. Fon. 2014. Parkin and PINK1 function in a vesicular trafficking pathway regulating mitochondrial quality control. *EMBO J.* 33:282-295.
- Meissner, C., H. Lorenz, A. Weihofen, D.J. Selkoe, and M.K. Lemberg. 2011. The mitochondrial intramembrane protease PARL cleaves human Pink1 to regulate Pink1 trafficking. *J Neurochem.* 117:856-867.
- Miyawaki, A., J. Llopis, R. Heim, J.M. McCaffery, J.A. Adams, M. Ikura, and R.Y. Tsien. 1997. Fluorescent indicators for Ca²⁺ based on green fluorescent proteins and calmodulin. *Nature.* 388:882-887.

- Morrison, E., J. Thompson, S.J. Williamson, M.E. Cheetham, and P.A. Robinson. 2011. A simple cell based assay to measure Parkin activity. *J Neurochem.* 116:342-349.
- Muller-Rischart, A.K., A. Pils, P. Beaudette, M. Patra, K. Hadian, M. Funke, R. Peis, A. Deinlein, C. Schweimer, P.H. Kuhn, S.F. Lichtenthaler, E. Motori, S. Hrelia, W. Wurst, D. Trumbach, T. Langer, D. Krappmann, G. Dittmar, J. Tatzelt, and K.F. Winklhofer. 2013. The E3 ligase parkin maintains mitochondrial integrity by increasing linear ubiquitination of NEMO. *Mol Cell.* 49:908-921.
- Narendra, D., A. Tanaka, D.F. Suen, and R.J. Youle. 2008. Parkin is recruited selectively to impaired mitochondria and promotes their autophagy. *J Cell Biol.* 183:795-803.
- Narendra, D.P., S.M. Jin, A. Tanaka, D.F. Suen, C.A. Gautier, J. Shen, M.R. Cookson, and R.J. Youle. 2010. PINK1 is selectively stabilized on impaired mitochondria to activate Parkin. *PLoS Biol.* 8:e1000298.
- Nicklas, W.J., I. Vyas, and R.E. Heikkila. 1985. Inhibition of NADH-linked oxidation in brain mitochondria by 1-methyl-4-phenyl-pyridine, a metabolite of the neurotoxin, 1-methyl-4-phenyl-1,2,5,6-tetrahydropyridine. *Life Sci.* 36:2503-2508.
- Okatsu, K., F. Koyano, M. Kimura, H. Kosako, Y. Saeki, K. Tanaka, and N. Matsuda. 2015. Phosphorylated ubiquitin chain is the genuine Parkin receptor. *J Cell Biol.* 209:111-128.
- Ordureau, A., S.A. Sarraf, D.M. Duda, J.M. Heo, M.P. Jedrychowski, V.O. Sviderskiy, J.L. Olszewski, J.T. Koerber, T. Xie, S.A. Beausoleil, J.A. Wells, S.P. Gygi, B.A. Schulman, and J.W. Harper. 2014. Quantitative proteomics reveal a feedforward mechanism for mitochondrial PARKIN translocation and ubiquitin chain synthesis. *Mol Cell.* 56:360-375.
- Pacelli, C., N. Giguere, M.J. Bourque, M. Levesque, R.S. Slack, and L.E. Trudeau. 2015. Elevated Mitochondrial Bioenergetics and Axonal Arborization Size Are Key Contributors to the Vulnerability of Dopamine Neurons. *Curr Biol.* 25:2349-2360.
- Park, J., S.B. Lee, S. Lee, Y. Kim, S. Song, S. Kim, E. Bae, J. Kim, M. Shong, J.M. Kim, and J. Chung. 2006. Mitochondrial dysfunction in *Drosophila* PINK1 mutants is complemented by parkin. *Nature.* 441:1157-1161.
- Pickrell, A.M., and R.J. Youle. 2015. The roles of PINK1, parkin, and mitochondrial fidelity in Parkinson's disease. *Neuron.* 85:257-273.
- Pissadaki, E.K., and J.P. Bolam. 2013. The energy cost of action potential propagation in dopamine neurons: clues to susceptibility in Parkinson's disease. *Front Comput Neurosci.* 7:13.
- Piston, D.W., and G.J. Kremers. 2007. Fluorescent protein FRET: the good, the bad and the ugly. *Trends Biochem Sci.* 32:407-414.
- Pollok, B.A., and R. Heim. 1999. Using GFP in FRET-based applications. *Trends Cell Biol.* 9:57-60.
- Potting, C., C. Crochemore, F. Moretti, F. Nigsch, I. Schmidt, C. Manneville, W. Carbone, J. Knehr, R. DeJesus, A. Lindeman, R. Maher, C. Russ, G. McAllister, J.S. Reece-Hoyes, G.R. Hoffman, G. Roma, M. Muller, A.W. Sailer, and S.B. Helliwell. 2018. Genome-wide CRISPR screen for PARKIN regulators reveals transcriptional repression as a determinant of mitophagy. *Proc Natl Acad Sci U S A.* 115:E180-E189.
- Salach, J.I., T.P. Singer, N. Castagnoli, Jr., and A. Trevor. 1984. Oxidation of the neurotoxic amine 1-methyl-4-phenyl-1,2,3,6-tetrahydropyridine (MPTP) by monoamine oxidases A and B and suicide inactivation of the enzymes by MPTP. *Biochem Biophys Res Commun.* 125:831-835.

- Sauve, V., A. Lilov, M. Seirafi, M. Vranas, S. Rasool, G. Kozlov, T. Sprules, J. Wang, J.F. Trempe, and K. Gehring. 2015. A Ubl/ubiquitin switch in the activation of Parkin. *EMBO J.* 34:2492-2505.
- Schapira, A.H., V.M. Mann, J.M. Cooper, D. Dexter, S.E. Daniel, P. Jenner, J.B. Clark, and C.D. Marsden. 1990. Anatomic and disease specificity of NADH CoQ1 reductase (complex I) deficiency in Parkinson's disease. *J Neurochem.* 55:2142-2145.
- Schapira, A.H.V., K.R. Chaudhuri, and P. Jenner. 2017. Non-motor features of Parkinson disease. *Nat Rev Neurosci.* 18:509.
- Shiba-Fukushima, K., Y. Imai, S. Yoshida, Y. Ishihama, T. Kanao, S. Sato, and N. Hattori. 2012. PINK1-mediated phosphorylation of the Parkin ubiquitin-like domain primes mitochondrial translocation of Parkin and regulates mitophagy. *Sci Rep.* 2:1002.
- Shin, J.H., H.S. Ko, H. Kang, Y. Lee, Y.I. Lee, O. Pletinkova, J.C. Troconso, V.L. Dawson, and T.M. Dawson. 2011. PARIS (ZNF746) repression of PGC-1alpha contributes to neurodegeneration in Parkinson's disease. *Cell.* 144:689-702.
- Siddiqui, A., D. Bhaumik, S.J. Chinta, A. Rane, S. Rajagopalan, C.A. Lieu, G.J. Lithgow, and J.K. Andersen. 2015. Mitochondrial Quality Control via the PGC1alpha-TFEB Signaling Pathway Is Compromised by Parkin Q311X Mutation But Independently Restored by Rapamycin. *J Neurosci.* 35:12833-12844.
- Simeonov, A., and M.I. Davis. 2004. Interference with Fluorescence and Absorbance. *In* Assay Guidance Manual. G.S. Sittampalam, N.P. Coussens, K. Brimacombe, A. Grossman, M. Arkin, D. Auld, C. Austin, J. Baell, B. Bejcek, T.D.Y. Chung, J.L. Dahlin, V. Devanaryan, T.L. Foley, M. Glicksman, M.D. Hall, J.V. Hass, J. Inglese, P.W. Iversen, S.D. Kahl, S.C. Kales, M. Lal-Nag, Z. Li, J. McGee, O. McManus, T. Riss, O.J. Trask, Jr., J.R. Weidner, M. Xia, and X. Xu, editors, Bethesda (MD).
- Soubannier, V., G.L. McLelland, R. Zunino, E. Braschi, P. Rippstein, E.A. Fon, and H.M. McBride. 2012. A vesicular transport pathway shuttles cargo from mitochondria to lysosomes. *Curr Biol.* 22:135-141.
- Spillantini, M.G., R.A. Crowther, R. Jakes, M. Hasegawa, and M. Goedert. 1998. alpha-Synuclein in filamentous inclusions of Lewy bodies from Parkinson's disease and dementia with lewy bodies. *Proc Natl Acad Sci U S A.* 95:6469-6473.
- Stevens, D.A., Y. Lee, H.C. Kang, B.D. Lee, Y.I. Lee, A. Bower, H. Jiang, S.U. Kang, S.A. Andrabi, V.L. Dawson, J.H. Shin, and T.M. Dawson. 2015. Parkin loss leads to PARIS-dependent declines in mitochondrial mass and respiration. *Proc Natl Acad Sci U S A.* 112:11696-11701.
- Stryer, L. 1978. Fluorescence energy transfer as a spectroscopic ruler. *Annu Rev Biochem.* 47:819-846.
- Tanaka, A., M.M. Cleland, S. Xu, D.P. Narendra, D.F. Suen, M. Karbowski, and R.J. Youle. 2010. Proteasome and p97 mediate mitophagy and degradation of mitofusins induced by Parkin. *J Cell Biol.* 191:1367-1380.
- Tang, M.Y., M. Vranas, A.I. Krahn, S. Pundlik, J.F. Trempe, and E.A. Fon. 2017. Structure-guided mutagenesis reveals a hierarchical mechanism of Parkin activation. *Nat Commun.* 8:14697.
- Tanner, C.M., F. Kamel, G.W. Ross, J.A. Hoppin, S.M. Goldman, M. Korell, C. Marras, G.S. Bhudhikanok, M. Kasten, A.R. Chade, K. Comyns, M.B. Richards, C. Meng, B. Priestley, H.H. Fernandez, F. Cambi, D.M. Umbach, A. Blair, D.P. Sandler, and J.W. Langston. 2011. Rotenone, paraquat, and Parkinson's disease. *Environ Health Perspect.* 119:866-872.

- Theile, C.S., M.D. Witte, A.E. Blom, L. Kundrat, H.L. Ploegh, and C.P. Guimaraes. 2013. Site-specific N-terminal labeling of proteins using sortase-mediated reactions. *Nat Protoc.* 8:1800-1807.
- Thrower, J.S., L. Hoffman, M. Rechsteiner, and C.M. Pickart. 2000. Recognition of the polyubiquitin proteolytic signal. *EMBO J.* 19:94-102.
- Trempe, J.F., V. Sauve, K. Grenier, M. Seirafi, M.Y. Tang, M. Menade, S. Al-Abdul-Wahid, J. Krett, K. Wong, G. Kozlov, B. Nagar, E.A. Fon, and K. Gehring. 2013. Structure of parkin reveals mechanisms for ubiquitin ligase activation. *Science.* 340:1451-1455.
- Truong, K., and M. Ikura. 2001. The use of FRET imaging microscopy to detect protein-protein interactions and protein conformational changes in vivo. *Curr Opin Struct Biol.* 11:573-578.
- Valente, E.M., S. Salvi, T. Ialongo, R. Marongiu, A.E. Elia, V. Caputo, L. Romito, A. Albanese, B. Dallapiccola, and A.R. Bentivoglio. 2004. PINK1 mutations are associated with sporadic early-onset parkinsonism. *Ann Neurol.* 56:336-341.
- Villace, P., R.M. Mella, M. Roura-Ferrer, M. Valcarcel, C. Salado, A. Castilla, and D. Kortazar. 2017. Fluorescent Parkin Cell-Based Assay Development for the Screening of Drugs against Parkinson Disease. *SLAS Discov.* 22:67-76.
- Wenzel, D.M., A. Lissounov, P.S. Brzovic, and R.E. Klevit. 2011. UBC7 reactivity profile reveals parkin and HHARI to be RING/HECT hybrids. *Nature.* 474:105-108.
- Xia, Z., and Y. Liu. 2001. Reliable and global measurement of fluorescence resonance energy transfer using fluorescence microscopes. *Biophys J.* 81:2395-2402.
- Xu, P., D.M. Duong, N.T. Seyfried, D. Cheng, Y. Xie, J. Robert, J. Rush, M. Hochstrasser, D. Finley, and J. Peng. 2009. Quantitative proteomics reveals the function of unconventional ubiquitin chains in proteasomal degradation. *Cell.* 137:133-145.
- Yamano, K., and R.J. Youle. 2013. PINK1 is degraded through the N-end rule pathway. *Autophagy.* 9:1758-1769.
- Yang, Y., S. Gehrke, Y. Imai, Z. Huang, Y. Ouyang, J.W. Wang, L. Yang, M.F. Beal, H. Vogel, and B. Lu. 2006. Mitochondrial pathology and muscle and dopaminergic neuron degeneration caused by inactivation of *Drosophila* Pink1 is rescued by Parkin. *Proc Natl Acad Sci U S A.* 103:10793-10798.
- Zhang, J.H., T.D. Chung, and K.R. Oldenburg. 1999. A Simple Statistical Parameter for Use in Evaluation and Validation of High Throughput Screening Assays. *J Biomol Screen.* 4:67-73.
- Zhou, C., Y. Huang, Y. Shao, J. May, D. Prou, C. Perier, W. Dauer, E.A. Schon, and S. Przedborski. 2008. The kinase domain of mitochondrial PINK1 faces the cytoplasm. *Proc Natl Acad Sci U S A.* 105:12022-12027.

Figures

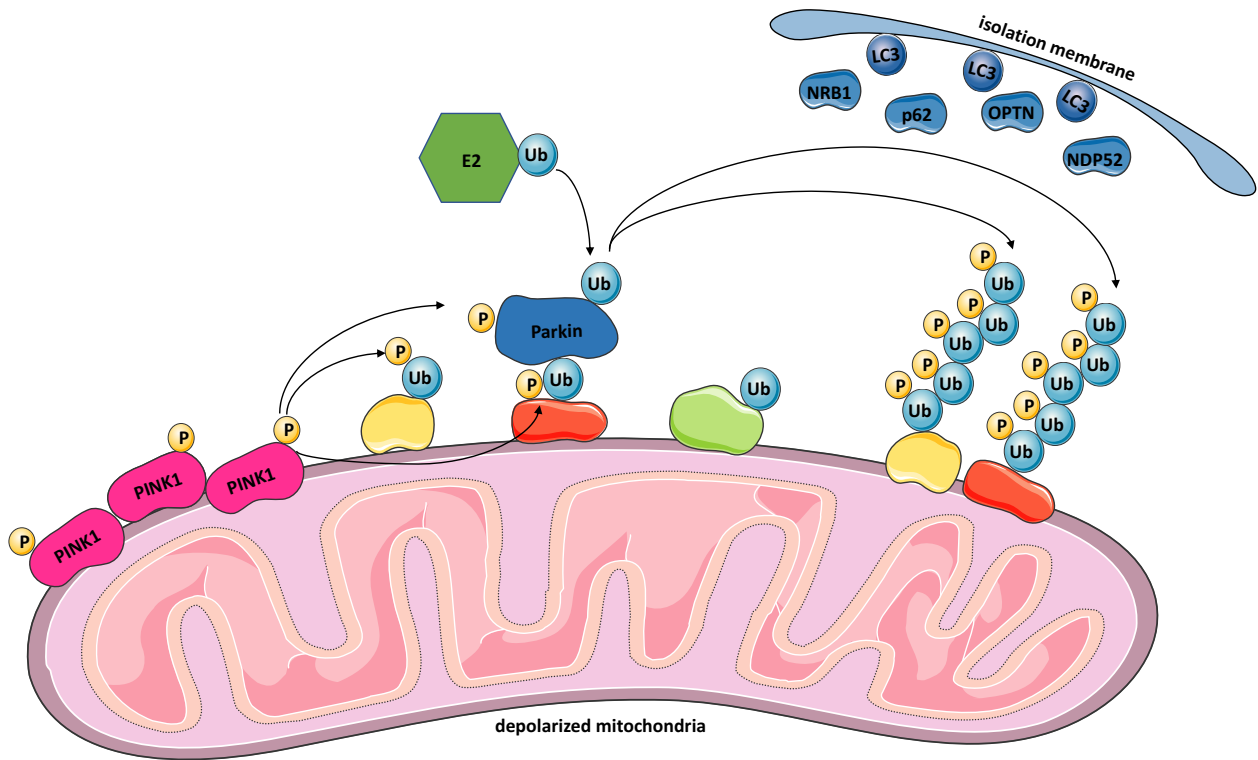


Figure 1. Model of PINK1/Parkin mediated mitophagy. Depolarization of mitochondria results in the accumulation of PINK1 on the outer membrane. PINK1 phosphorylates Ub bound to mitochondrial proteins, which results in the recruitment of Parkin from the cytoplasm. pUb binds Parkin, inducing allosteric changes that make the Ub1 more accessible for phosphorylation by PINK1 at a conserved Ser65 residue. Parkin binds to the E2 Ub-conjugating enzyme and transfers the Ub onto its substrate via a thioester intermediate at its catalytic Cys431. Ubiquitinated mitochondrial fusion proteins Mfn1 and Mfn2 are then degraded by the proteasome, resulting in a reduction of mitochondrial fusion. Ub chains on substrates not targeted for proteasomal degradation can be phosphorylated by PINK1, triggering a feed-forward amplification of Parkin translocation to the mitochondria. Polyubiquitinated mitochondrial substrates also recruit autophagy adaptor proteins such as NBR1, p62, NDP52, and OPTN, which interact with LC3 to engulf the entire organelle into an autophagosome that will fuse with the lysosome for degradation.

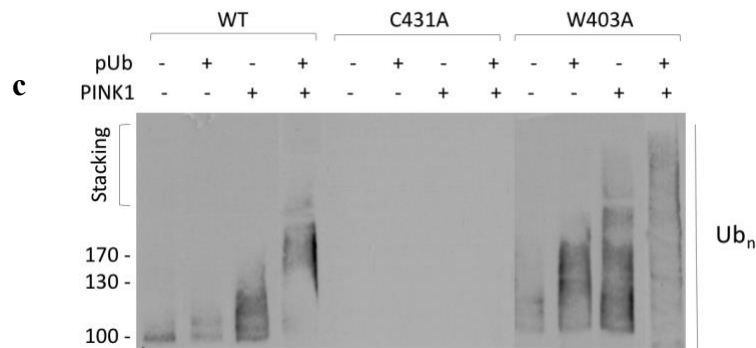
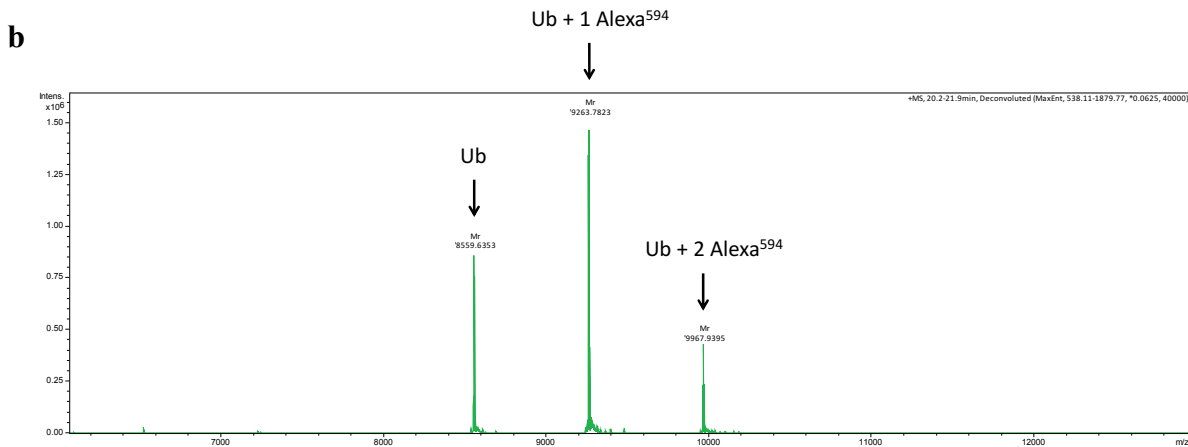
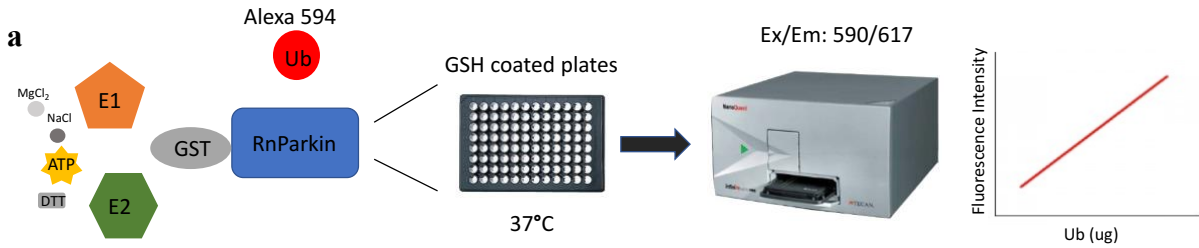


Figure 2. Auto-ubiquitination assay. (a) Schematic diagram of assay. GST-*RnParkin* is immobilized on GSH-coated black plates, to which the components necessary for transfer of Ub onto Parkin are added. Plates are incubated at 37°C for a determined amount of time and thoroughly rinsed thereafter. The plates can then be placed in a fluorescence plate reader. The more labelled Ub is bound onto the immobilized GST-*RnParkin*, the higher fluorescence intensity is observed. Certain variables such as longer time points, as well as addition of pUb or PINK1, increase the amount of polyubiquitin chains Parkin will form. (b) Mass spectrometry showed Ub was predominantly labelled with only one molecule of Alexa 594. (c) Ub labelled with Alexa 594 was able to form polyubiquitin chains on Parkin. Conditions such as an activating mutation (W403A) or the addition of pUb and PINK1 result in the formation of longer polyubiquitin chains.

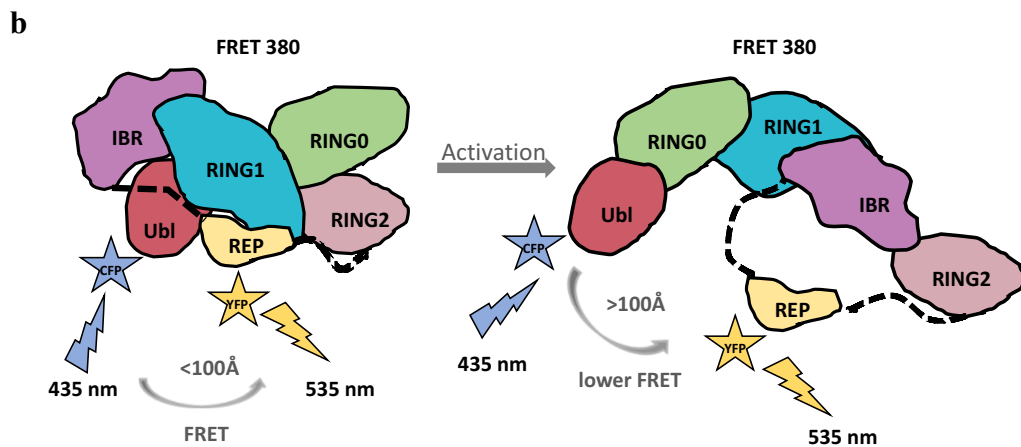
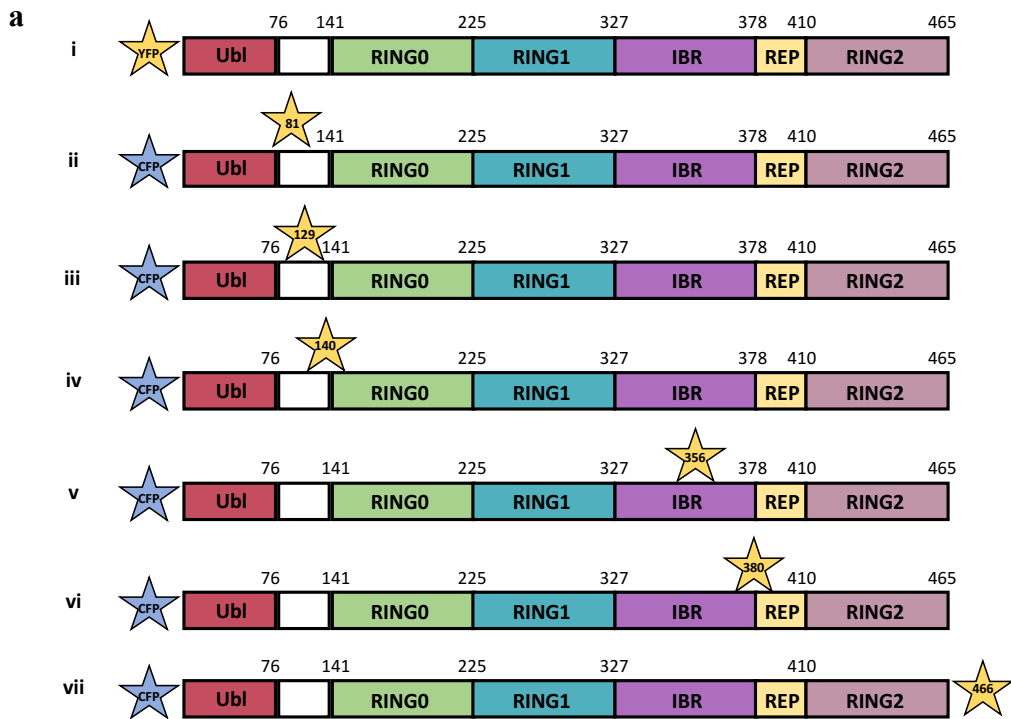


Figure 3. FRET assay. (a) Diagram of FRET reporter constructs showing Parkin tagged with the donor CFP at its N-terminus and the acceptor Venus (YFP) at different positions. (b) Under basal conditions, both fluorescent proteins are within close enough proximity to give a FRET signal. During activation, Parkin adopts a different conformation, resulting in a decrease of FRET efficiency as both fluorescent proteins move further away from each other.

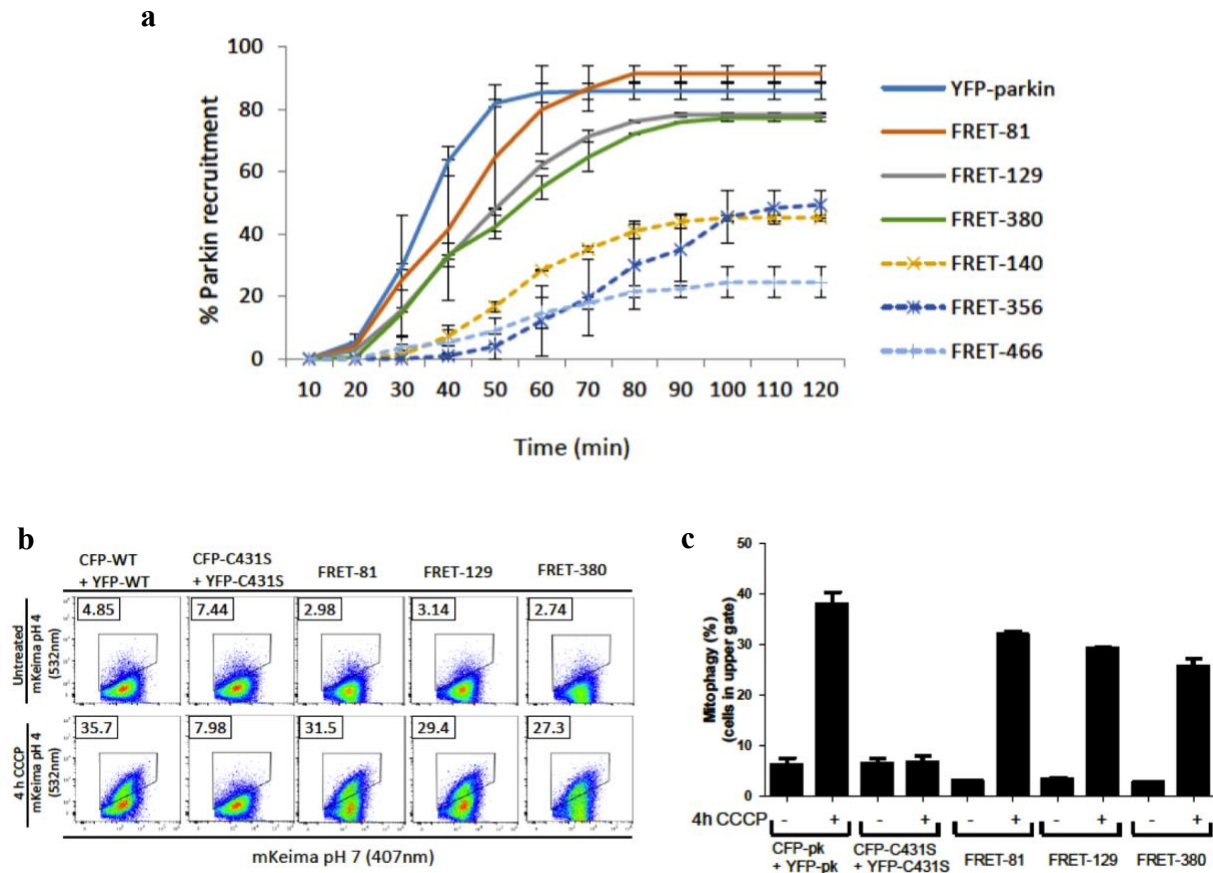


Figure 4. Kinetics and activity of FRET reporters. (a) FRET constructs were tested in a mitochondrial recruitment assay following addition of CCCP to ensure that the inserted fluorescent proteins did not interfere with the function of the protein. HeLa cells were transiently transfected with either YFP-Parkin or various FRET reporters. The percentage of cells showing recruitment of FRET-Parkin reporters to the mitochondria was determined every 10 min over a period of 120 min. FRET-140, FRET-356, and FRET-466 had delayed recruitment and were, therefore; not further analyzed. Error bars represent SEM from two independent experiments. (b) FACS-based mitophagy assay showed no impairment of mitophagy for the FRET constructs. Representative data of U2OS cells stably expressing mtKeima that were transfected with FRET reporters and treated with CCCP for 4 h. Cells co-transfected with CFP-WT and YFP-WT, or CFP-C431S and YFP-C431S served as positive and negative controls, respectively. (c) Quantification of average percent mitophagy. Error bars represent SEM from two independent experiments.

*Figures were adapted from Tang, et al., 2017.

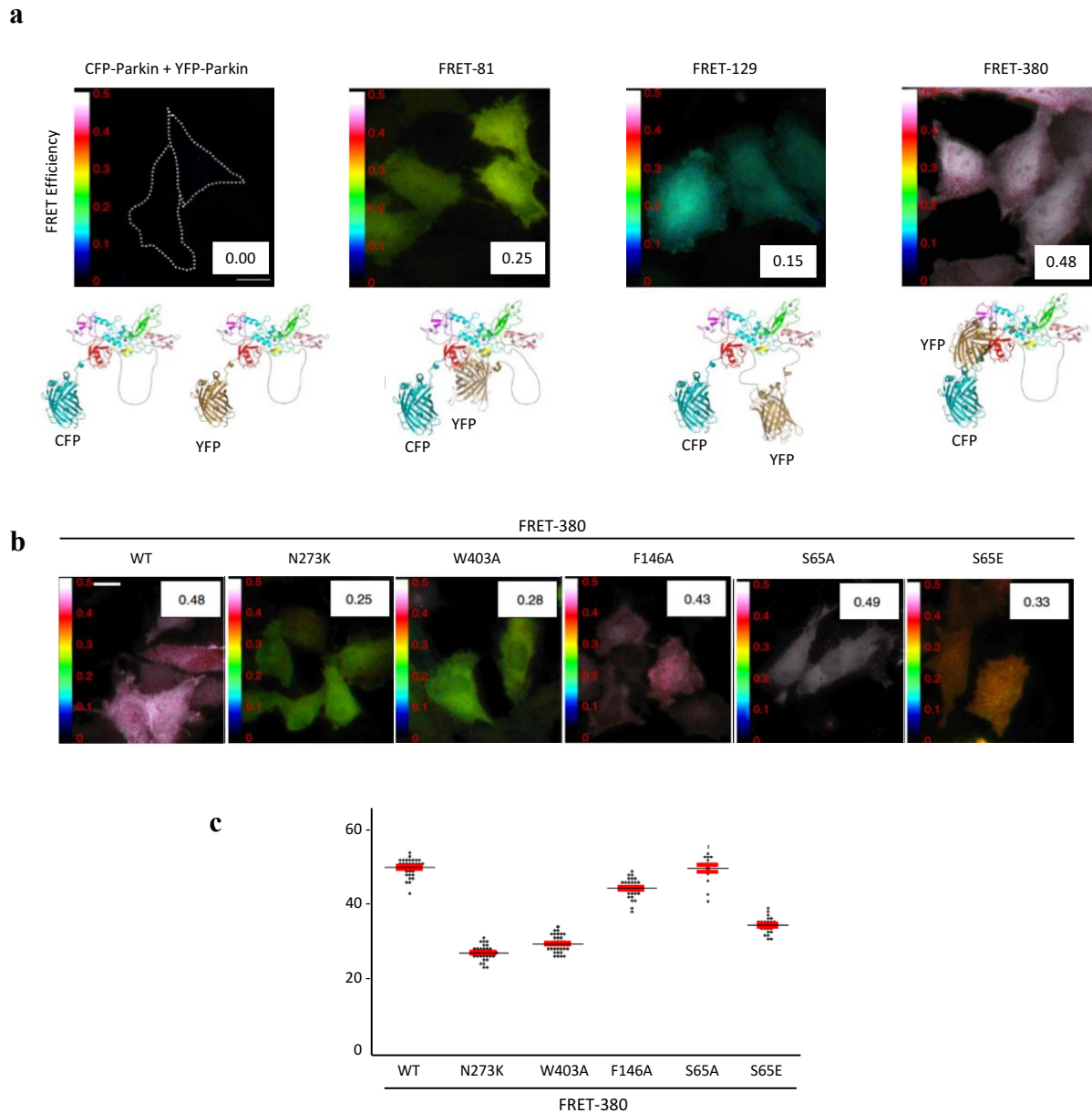


Figure 5. Changes in FRET efficiencies. (a) Representative images of HeLa cells that were transiently transfected with FRET constructs. Average FRET efficiencies are indicated at the bottom right corner of each image. A colour-coded FRET map with a scale ranging from 0.00 to 0.50 displays FRET ratios (warm colours represent higher FRET efficiencies while cooler colours represent lower FRET efficiencies). FRET efficiencies correlate with the distance between CFP and YFP in the molecular models derived from the crystal structure of Parkin. FRET constructs that have CFP and YFP in closer proximity have higher FRET efficiency than those with their fluorescent proteins further away from each other. (b) Representative images of HeLa cells transfected with FRET-380 and its variants. Average FRET efficiencies are indicated at the top right corner of each image. (c) Quantification of FRET efficiency measurements from b. Activating mutations show a decrease in FRET efficiency for FRET-380. Each data point represents the FRET efficiency measurement from one cell.

*Figures were adapted from Tang, et al., 2017.

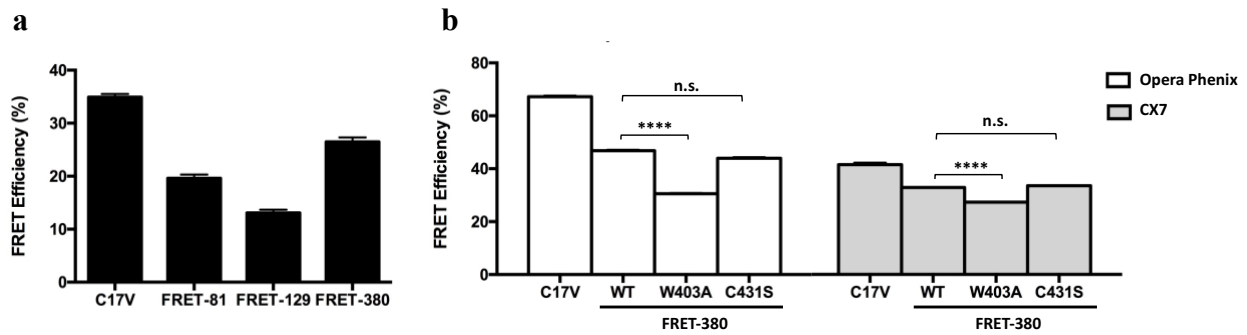


Figure 6. Testing FRET reporters for high-content screening. (a) U2OS cells stably expressing FRET constructs were tested on a fluorescence plate reader. C17V (cerulean attached via a 17aa linker to Venus) was used as a positive control. The values obtained from the plate reader followed the same trend that was observed with the transiently transfected Hela cells on the fluorescence microscope, with FRET-380 displaying the highest FRET efficiency and FRET-129 having the lowest FRET efficiency. Error bars represent SEM from two independent experiments. (b) U2OS cells stably expressing FRET-380 were tested on two high content microscopes: Opera Phenix HCS System (Perkin Elmer) and CellInsight CX7 HCS Platform (Thermo Fisher). W403A and C431S were used as positive and negative controls, respectively. Error bars represent SEM from two independent experiments; **** $P < 0.0001$; n.s., nonsignificant (one-way ANOVA with Dunnett's test).

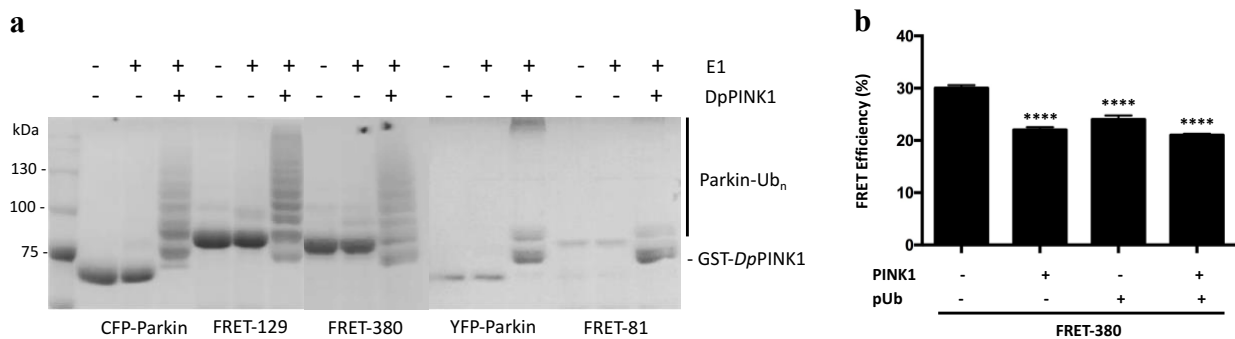
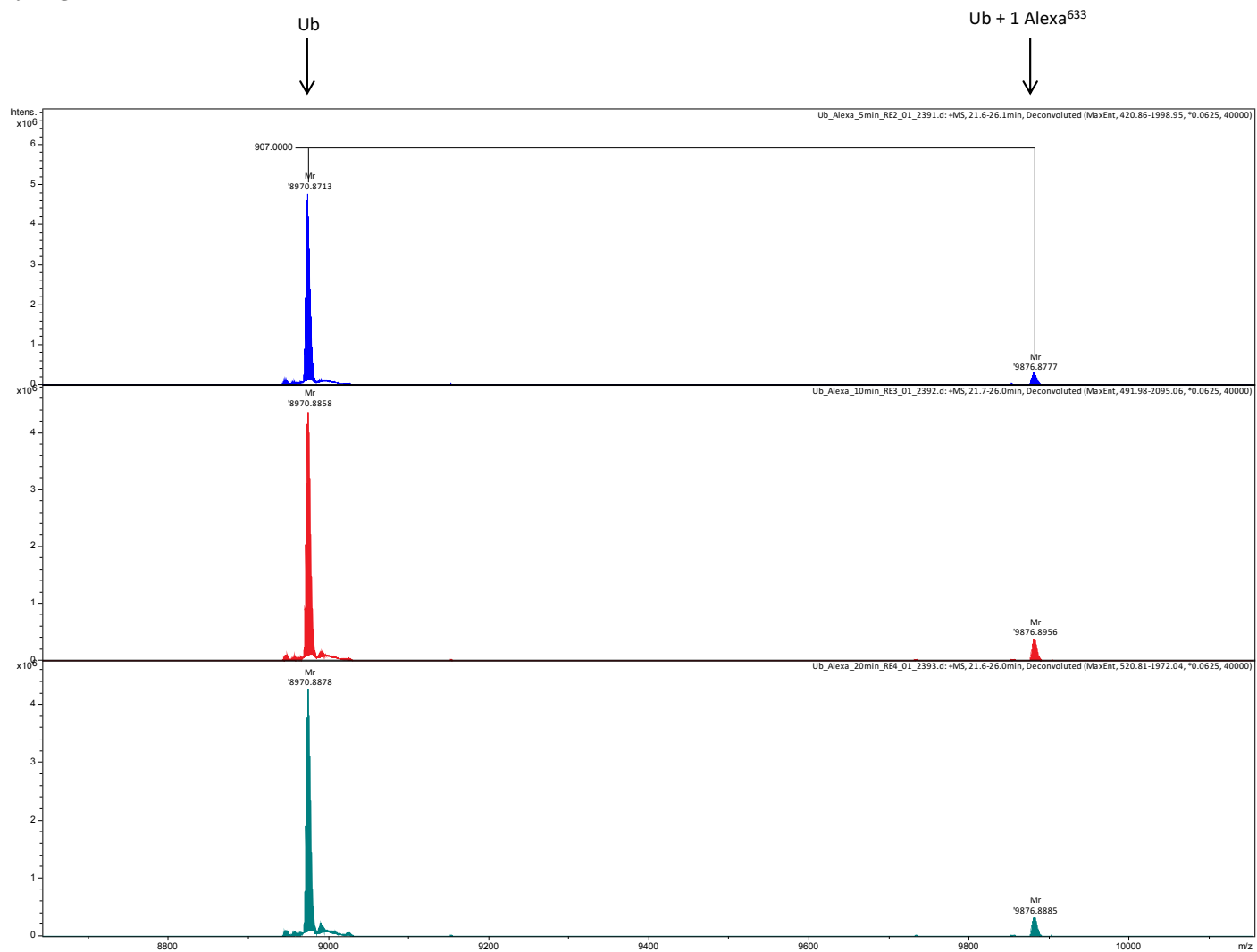
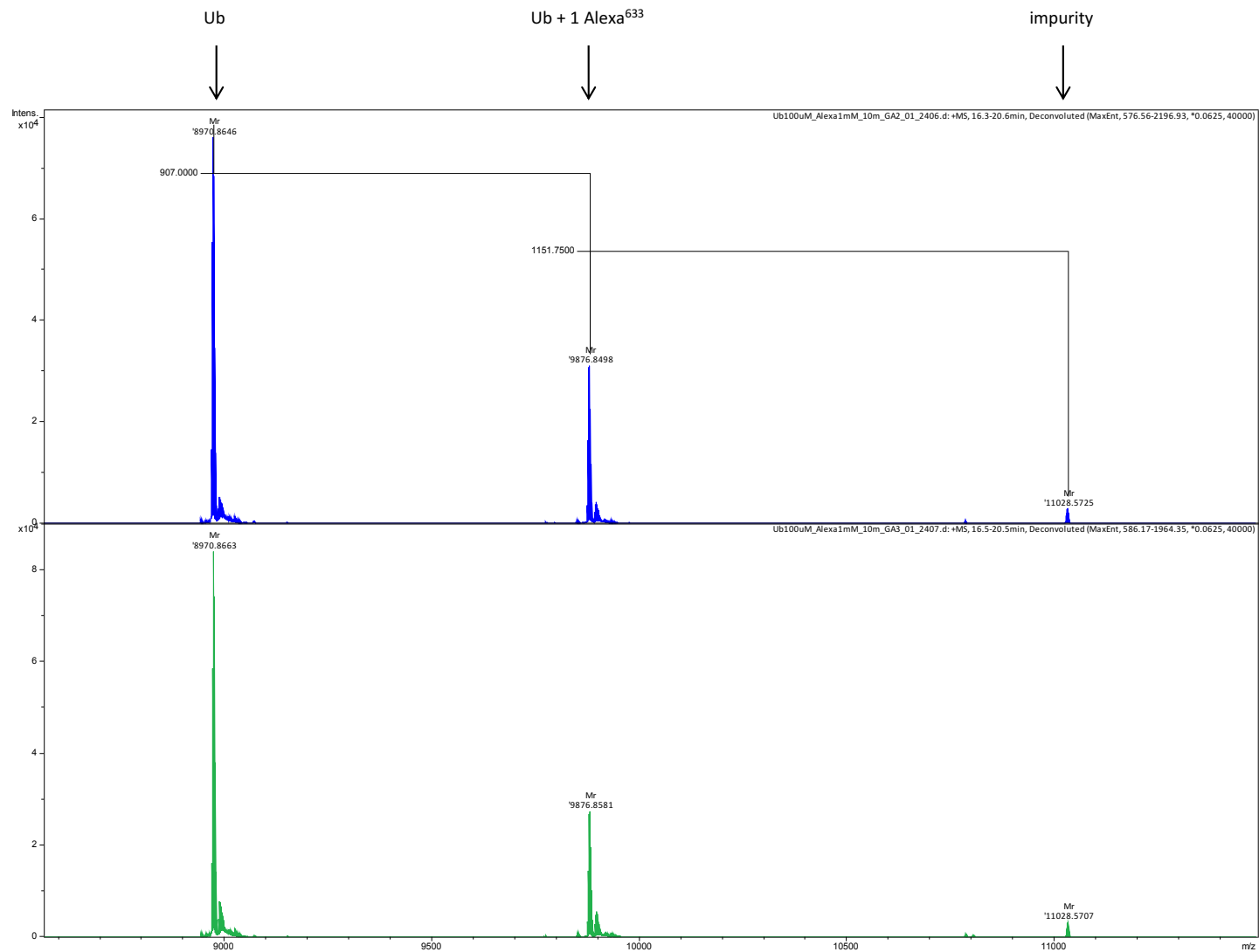


Figure 7. Modified *in vitro* FRET assay. (a) *In vitro* auto-ubiquitination assay confirmed purified recombinant *HsParkin* FRET reporter proteins are stable and are susceptible to activation by phosphorylation by PINK1. *Figure was adapted from Tang, et al., 2017. (b) Addition of pUb and/or PINK1 decrease FRET efficiency in our recombinant FRET-380 protein. Error bars represent SEM from two independent experiments. **** $P < 0.0001$ (one-way ANOVA with Dunnett's test).

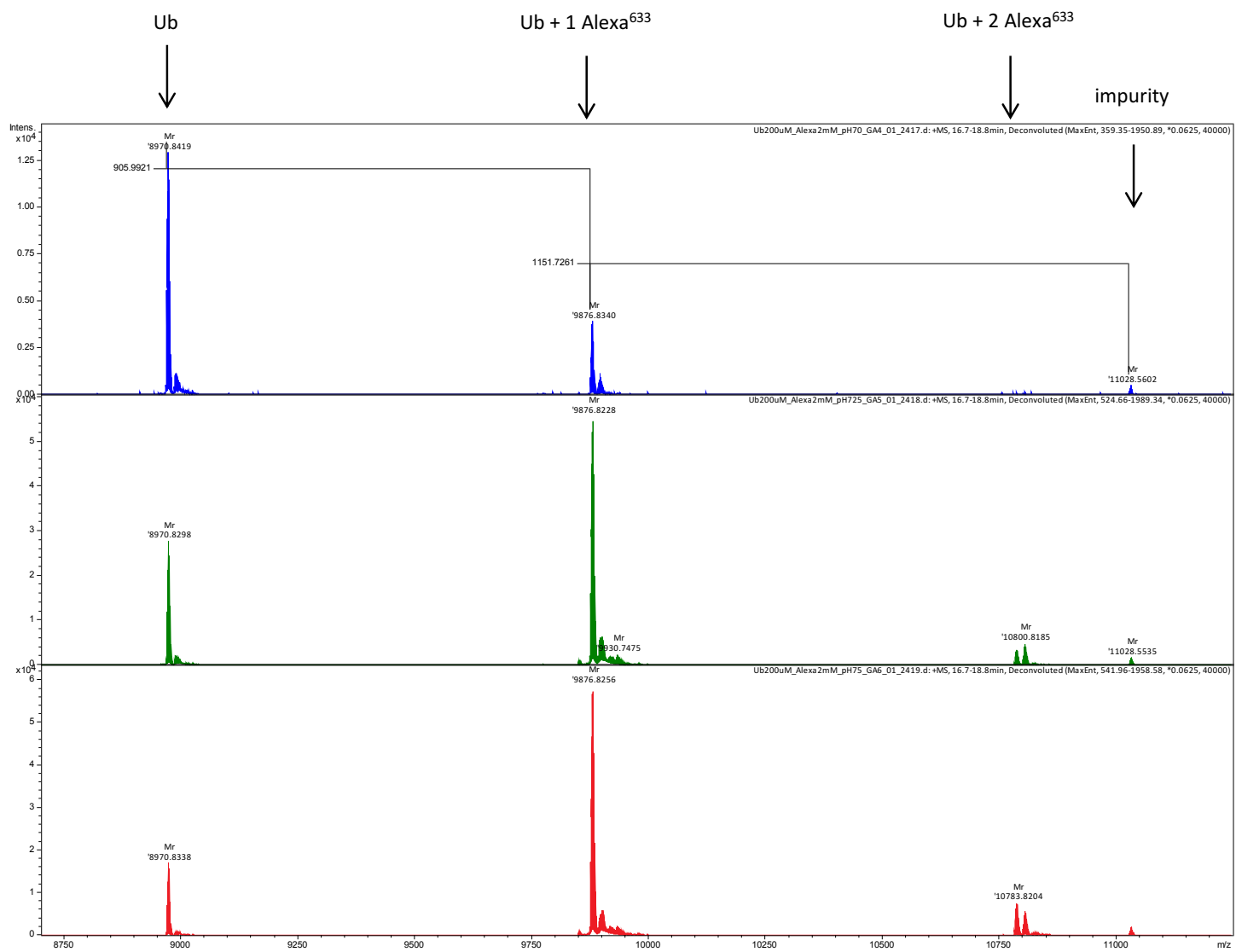
Supplementary Figures



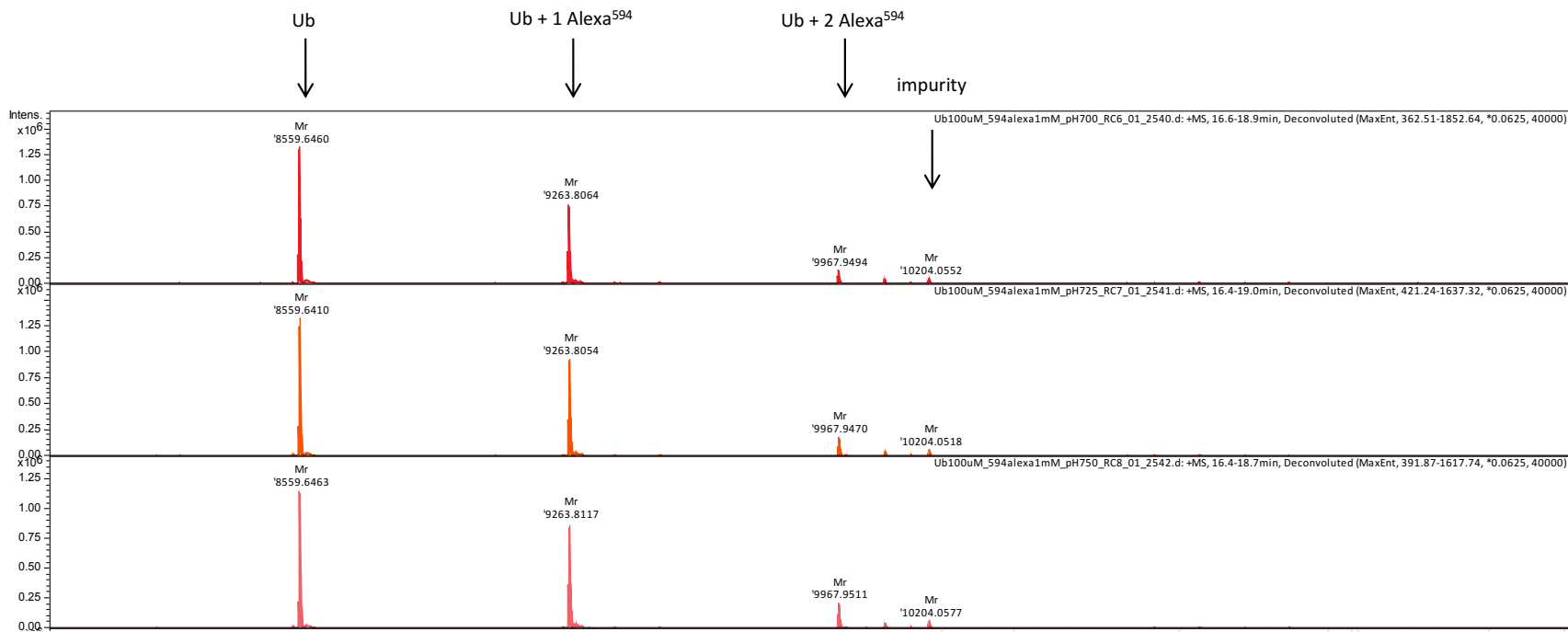
Supplementary Figure 1. Determining labelling duration. Mass spectrometry showed no change for 5 min (blue), 10 min (red), or 20 min (green) with 2:1 Alexa⁶³³:Ub, suggesting the reaction was complete within the first 5 min. Only ~5% of Ub was labelled with the chosen 2:1 molar ratio.



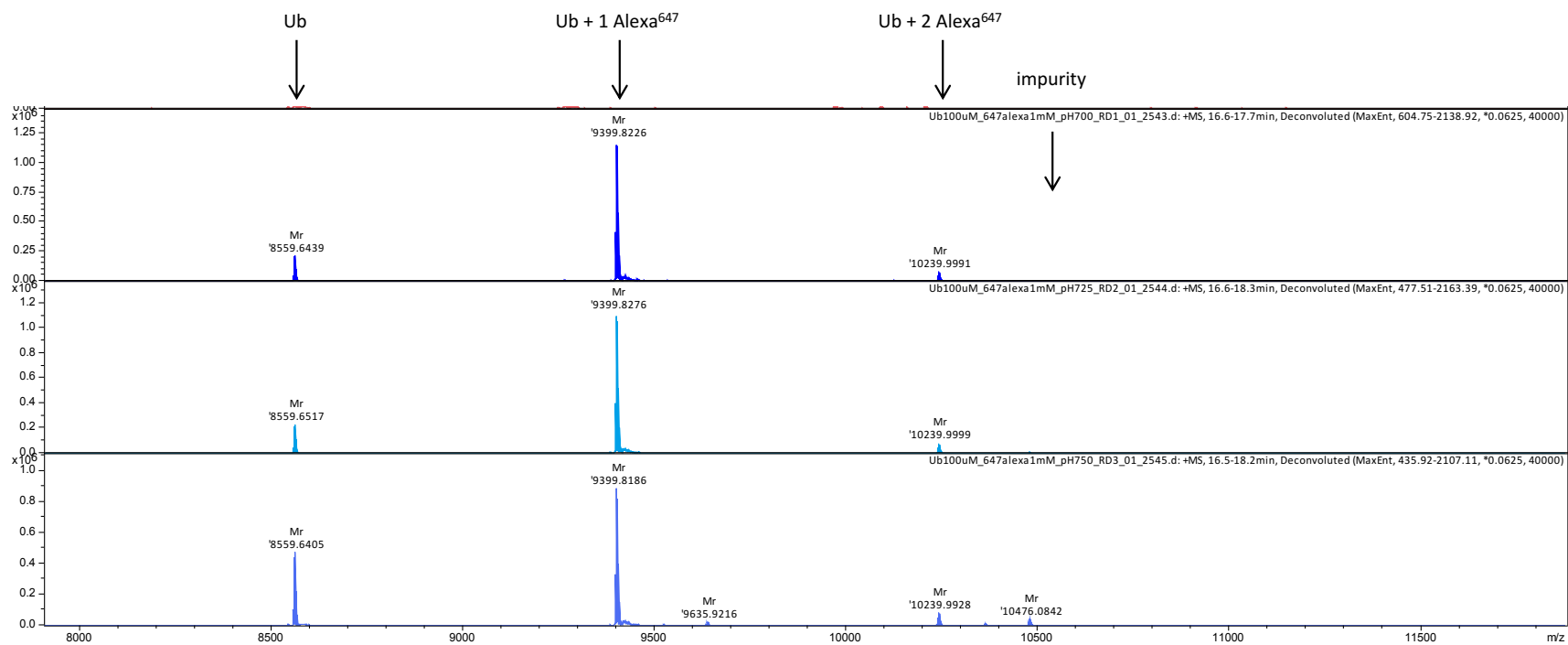
Supplementary Figure 2. Determining labelling molar ratio. Mass spectrometry showed ~30% labelling with 10:1 Alexa⁶³³:Ub (blue) vs ~25% labelling with 5:1 Alexa⁶³³:Ub (green).



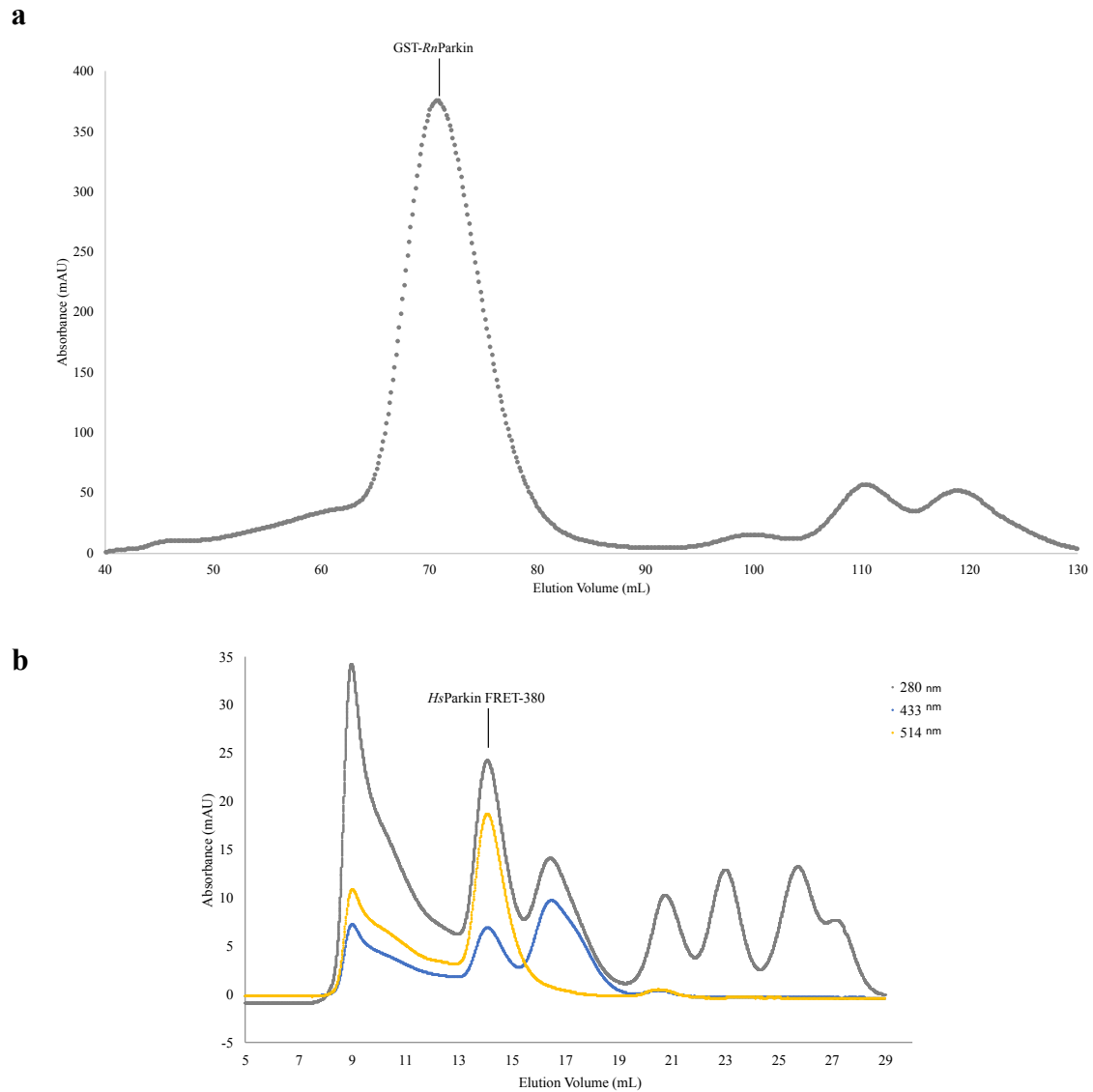
Supplementary Figure 3. Determining labelling pH. Mass spectrometry showed labelling of Ub with only one molecule of Alexa⁶³³ at pH 7.00 (blue), while double labelling occurred at pH 7.25 (green) and pH 7.50 (red) with 10:1 Alexa⁶³³:Ub.



Supplementary Figure 4. Determining labelling pH. Mass spectrometry traces of 10:1 Alexa⁵⁹⁴:Ub at pH 7.00 (top), pH 7.25 (middle), and pH 7.50 (bottom). More double labelling occurred with increasing pH.



Supplementary Figure 5. Determining labelling pH. Mass spectrometry traces of 10:1 Alexa⁶⁴⁷:Ub at pH 7.00 (top), pH 7.25 (middle), and pH 7.50 (bottom). Higher amounts of unlabelled Ub were observed with increasing pH.



Supplementary Figure 8. FPLC gel filtration separation of recombinant proteins. (a) FPLC trace for GST-*RnParkin* during gel filtration at an absorbance of 280 nm. **(b)** FPLC trace for *HsParkin* FRET-380 (280 nm, grey; 433 nm, blue; 514 nm, yellow).